


國立臺灣大學電機資訊學院電信工程學研究所

碩士論文

Graduate Institute of Communication Engineering  
College of Electrical Engineering and Computer Science  
National Taiwan University

Master Thesis

正交分頻多工系統中實虛部非協調與載波頻率位移之同估測  
Joint Estimation of I/Q Imbalance and Carrier Frequency Offset  
for OFDM Systems

The image features a large, faint watermark of the National Taiwan University seal in the background. The seal is circular and contains the university's name in Chinese characters: '國立臺灣大學' at the top, '電機資訊學院' on the left, and '電信工程學研究所' on the right. In the center of the seal is a bell, and below it, the motto '敦品 勵學 健體' is written. The author's name '江威儒' is printed in the center of the seal, overlapping the bell and the motto.

江威儒

Wei-Ju Chiang

指導教授：馮世邁 博士

Advisor: See-May Phoong, Ph.D.

中華民國 100 年 6 月

June, 2011

JOINT ESTIMATION OF I/Q IMBALANCE AND  
CARRIER FREQUENCY OFFSET FOR OFDM SYSTEMS



By  
Wei-Ju Chiang

SUBMITTED IN PARTIAL FULFILLMENT OF THE  
REQUIREMENTS FOR THE DEGREE OF  
MASTER OF COMMUNICATION ENGINEER  
AT

NATIONAL TAIWAN UNIVERSITY

TAIPEI, TAIWAN

JULY 2011

© Copyright by Wei-Ju Chiang , 2011

NATIONAL TAIWAN UNIVERSITY

Date: July 2011

Author: Wei-Ju Chiang

Title: Joint Estimation of I/Q Imbalance and Carrier  
Frequency Offset for OFDM Systems

Department: Graduate Institute of Communication Engineering

Degree: M.Sc. Convocation: June Year: 2010

Permission is herewith granted to National Taiwan University to circulate and to have copied for non-commercial purposes, at its discretion, the above title upon the request of individuals or institutions.



---

Signature of Author

THE AUTHOR RESERVES OTHER PUBLICATION RIGHTS, AND NEITHER THE THESIS NOR EXTENSIVE EXTRACTS FROM IT MAY BE PRINTED OR OTHERWISE REPRODUCED WITHOUT THE AUTHOR'S WRITTEN PERMISSION.

THE AUTHOR ATTESTS THAT PERMISSION HAS BEEN OBTAINED FOR THE USE OF ANY COPYRIGHTED MATERIAL APPEARING IN THIS THESIS (OTHER THAN BRIEF EXCERPTS REQUIRING ONLY PROPER ACKNOWLEDGEMENT IN SCHOLARLY WRITING) AND THAT ALL SUCH USE IS CLEARLY ACKNOWLEDGED.

*To my family and friends.*



# Contents

List of Figures	vii
Abstract	ix
Acknowledgements	xi
<b>1 Introduction</b>	<b>1</b>
<b>2 I/Q Imbalance and Carrier Frequency Offset in OFDM Systems</b>	<b>5</b>
2.1 Introduction to OFDM Systems	6
2.2 The Phenomenon of I/Q Imbalance and CFO	10
2.2.1 I/Q Imbalance	12
2.2.2 Carrier Frequency offset	12
2.3 I/Q Imbalance and CFO on the Received Baseband Signal Model	13
2.4 Compensation of I/Q Imbalance and CFO	16
2.5 Simulation Result and Comparison	18
2.6 Concluding Remark	22
<b>3 Estimation and Compensation of CFO and I/Q imbalance</b>	<b>23</b>
3.1 Pilot Aided Compensation for CFO and I/Q Imbalance by GPP method	24
3.2 CFO Estimation by Three-Block method	27
3.3 Simulation Results	30
3.4 Concluding Remark	34

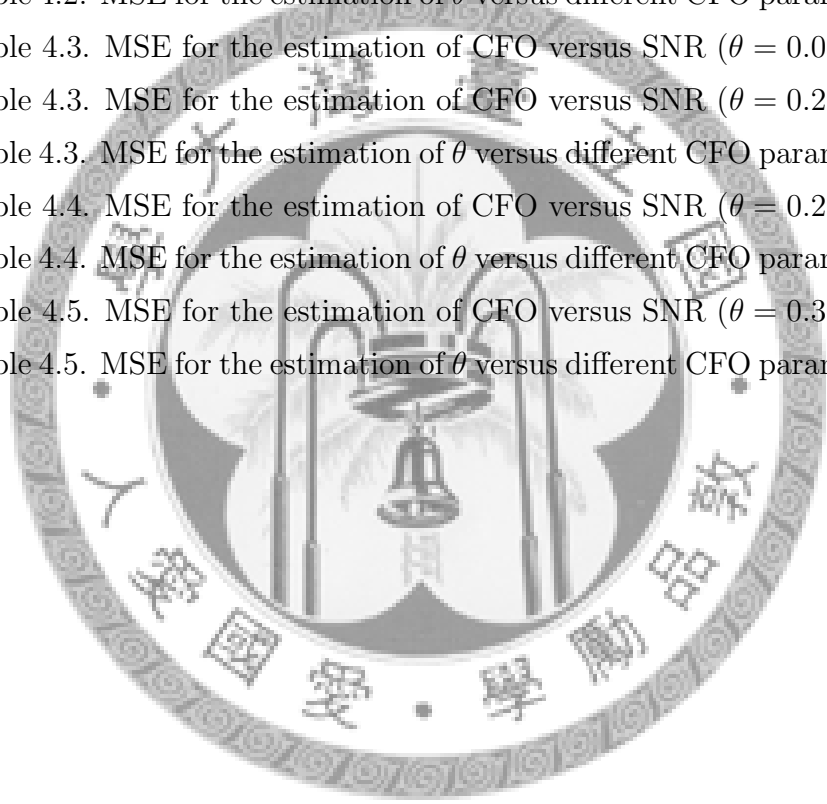
<b>4</b>	<b>Joint Estimation of I/Q Imbalance and CFO for OFDM system</b>	<b>35</b>
4.1	Proposed Joint Estimation Method of CFO and I/Q Imbalance . . . . .	36
4.1.1	CFO Estimation . . . . .	37
4.1.2	I/Q Imbalance Estimation . . . . .	40
4.2	Improved of GPP Method . . . . .	42
4.3	Improved of Three-Block method . . . . .	44
4.4	Simulation Results and Comparison . . . . .	47
4.5	Concluding Remark . . . . .	57
<b>5</b>	<b>Conclusion</b>	<b>59</b>
	<b>Bibliography</b>	<b>61</b>



# List of Figures

2.1	Block diagram of OFDM system . . . . .	7
2.2	Idea direct-conversion receiver . . . . .	11
2.3	Arithmetic model for DCR with I/Q imbalance and CFO . . . . .	13
2.4	A block diagram of OFDM with I/Q imbalance and CFO . . . . .	15
2.5	compensation structure for I/Q imbalance and CFO proposed in [12]	17
2.6	Example 2.1. Effect of I/Q imbalance on BER performance of OFDM systems . . . . .	20
2.7	Example 2.2. Effect of CFO on BER performance of OFDM systems	21
2.8	Example 2.3. Joint effect of CFO and I/Q imbalance on BER performance of OFDM systems . . . . .	22
3.1	Generalized periodic pilot . . . . .	24
3.2	compensation structure for I/Q imbalance and CFO . . . . .	25
3.3	Training sequences of Three-Block method . . . . .	28
3.4	$y = \arccos(x)$ . . . . .	30
3.5	Example 3.1. MSE for the estimation of $\theta$ versus different CFO parameter	32
3.6	Example 3.1. MSE for the estimation of compensation parameter versus different CFO parameter . . . . .	33
3.7	Example 3.2. MSE for the estimation of $\theta$ versus different CFO parameter	34
4.1	Training sequence of proposed method . . . . .	37
4.2	The data flow diagram for proposed joint estimation of CFO and I/Q imbalance in Sec.4.1 . . . . .	42

4.3	The data flow diagram for Improved of CFO Estimation by Using Three Repeated OFDM Blocks in Sec.4.3 . . . . .	46
4.4	Example 4.1. MSE for the estimation of CFO versus SNR ( $\theta = 0.3072$ )	48
4.5	Example 4.1. MSE for the estimation of $\theta$ versus different CFO parameter	49
4.6	Example 4.2. MSE for the estimation of CFO versus SNR ( $\theta = 0.02$ )	50
4.7	Example 4.2. MSE for the estimation of CFO versus SNR ( $\theta = 0.2$ ) .	50
4.8	Example 4.2. MSE for the estimation of $\theta$ versus different CFO parameter	51
4.9	Example 4.3. MSE for the estimation of CFO versus SNR ( $\theta = 0.02$ )	52
4.10	Example 4.3. MSE for the estimation of CFO versus SNR ( $\theta = 0.2$ ) .	52
4.11	Example 4.3. MSE for the estimation of $\theta$ versus different CFO parameter	53
4.12	Example 4.4. MSE for the estimation of CFO versus SNR ( $\theta = 0.2$ ) .	54
4.13	Example 4.4. MSE for the estimation of $\theta$ versus different CFO parameter	55
4.14	Example 4.5. MSE for the estimation of CFO versus SNR ( $\theta = 0.3072$ )	56
4.15	Example 4.5. MSE for the estimation of $\theta$ versus different CFO parameter	56

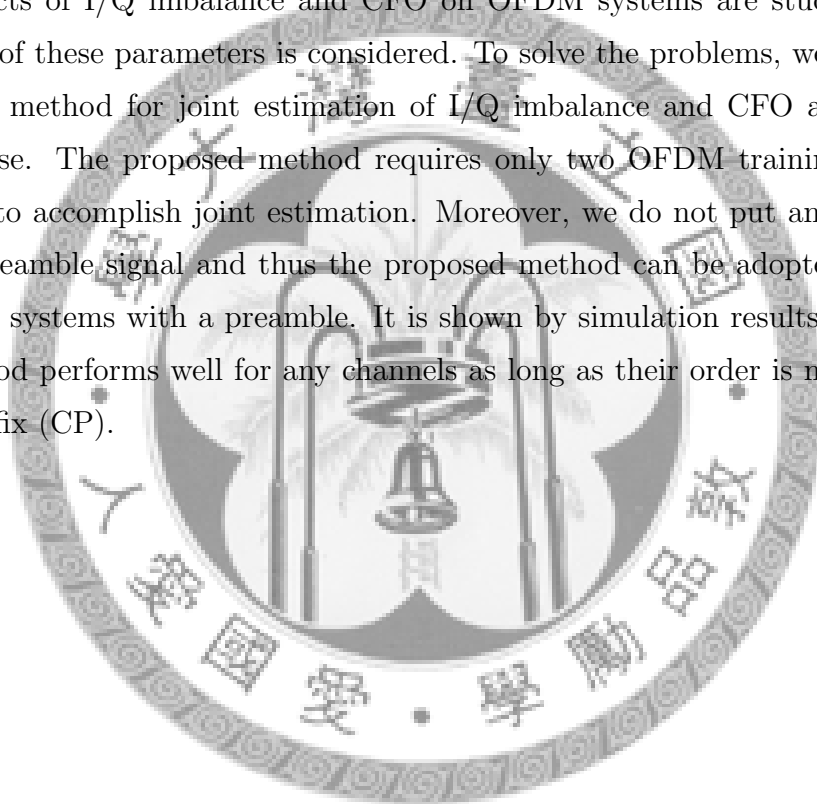




# Abstract



Nowadays, direct-conversion radio frequency (RF) receivers become more appealing. However, orthogonal frequency division multiplexing (OFDM) systems with direct-conversion RF receivers are very sensitive to non-idealities at the front-end of receiver, such as I/Q imbalance and carrier frequency offset (CFO). These non-idealities at the receiver result in inter-carrier interference (ICI). Accurate estimates of the non-idealities and channel response are required in OFDM systems. In this thesis, the effects of I/Q imbalance and CFO on OFDM systems are studied, and the estimation of these parameters is considered. To solve the problems, we propose a time domain method for joint estimation of I/Q imbalance and CFO as well as channel response. The proposed method requires only two OFDM training blocks as a preamble to accomplish joint estimation. Moreover, we do not put any restrictions on the preamble signal and thus the proposed method can be adopted in any communication systems with a preamble. It is shown by simulation results that our proposed method performs well for any channels as long as their order is not longer than cyclic prefix (CP).



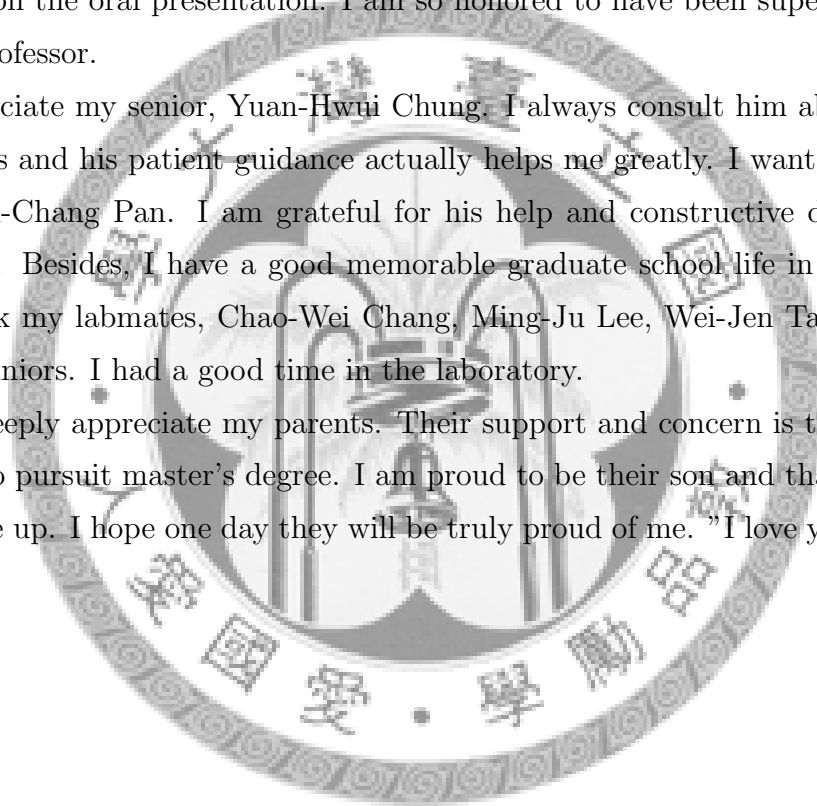
# Acknowledgements



I would like to express my immense gratitude to my supervisor, Dr. See-May Phoong, for his patient and helpful guidance throughout my research in this thesis. During these two years, he spent a lot of time on instructing me how to solve the problems and mistakes that I made and giving me insightful suggestions. More importantly, I learned what right attitude I should have from the process of thesis research. I appreciate him for reading the manuscript of my thesis and giving me helpful advice on the oral presentation. I am so honored to have been supervised by such a great professor.

I also appreciate my senior, Yuan-Hwui Chung. I always consult him about academic questions and his patient guidance actually helps me greatly. I want to thank my senior, Yen-Chang Pan. I am grateful for his help and constructive discussion in my research. Besides, I have a good memorable graduate school life in B.L 506. I want to thank my labmates, Chao-Wei Chang, Ming-Ju Lee, Wei-Jen Tai, Yi-Fan Jian and the juniors. I had a good time in the laboratory.

Finally, I deeply appreciate my parents. Their support and concern is the source of my energy to pursuit master's degree. I am proud to be their son and thank them for breeding me up. I hope one day they will be truly proud of me. "I love you, Mom and Dad"



# Chapter 1

## Introduction



Orthogonal frequency division multiplexing (OFDM) is a widely recognized and standardized modulation technique for broadband wireless communication systems such as IEEE 802.11 a/g, wireless local-area networks (Wi-Fi), high-speed digital subscriber lines (DSL), digital audio broadcasting (DAB) [1], and digital video broadcasting (DVB-T) [2]. Recently, direct-conversion radio frequency (RF) receivers become more attractive because of their significant advantages in cost, package size, and power consumption [3], [4]. However, OFDM systems are very sensitive to non-idealities at the front-end of receiver, such as I/Q imbalance and carrier frequency offset (CFO), etc. The non-idealities caused by I/Q imbalance, CFO, at the receiver result in inter-carrier interference (ICI), and the performance of OFDM systems degrades severely. Therefore, a precise scheme of estimation and compensation is essential for OFDM systems.

A large number of schemes compensating I/Q imbalance and CFO have been proposed in numerous literatures. In [12], a joint CFO and I/Q mismatches estimator, which needs at least two identical symbols is derived. It estimates CFO parameter by one-dimensional search at the first step. I/Q imbalances are estimated by solving an close form equation at the second step. In [13], a close form of both CFO and I/Q estimator is proposed by using least square method. [13] needs at least three identical symbols [15]. In [14], a close form is proposed when both CFO and frequency independent I/Q imbalance are present. [14] also needs at least three identical symbols.

In this thesis, we concentrate on joint estimation of I/Q imbalance, CFO and channel impulse response, and propose a time domain method to be applied for OFDM. In each transmission, a known preamble is first sent for joint estimation, then these estimated information can be used for the following data transmission. For systems such as IEEE 802.11a and IEEE 802.11g, the repeated preamble used for channel estimation in standard OFDM systems can be used for our joint estimation method, and our method only requires one OFDM training block as a preamble to accomplish joint estimation of all unknown parameters.

The rest of this thesis will be organized as follows. In chapter 2, we build a general

model of I/Q imbalance and CFO. Comprehend the impact on the received baseband signal and the BER performance. In chapter 3, We review some estimation methods for CFO and I/Q mismatches. In chapter 4, We proposed an joint estimation method for CFO and I/Q mismatches and improve the approaches introduced in chapter3. Simulation examples are given in each section. Finally, in chapter 5, we summarize the main conclusions obtained in this thesis.

**Notation** : Boldfaced letters are used to denote vectors and matrices. The symbols  $\mathbf{A}^T$ ,  $\mathbf{A}^H$  and  $\mathbf{A}^*$  denote the transpose, Hermitian and conjugate of  $\mathbf{A}$  respectively. The symbols  $\mathbf{A}^{-1}$  and  $\mathbf{A}^\dagger$  denote the inverse and the pseudo-inverse of  $\mathbf{A}$  respectively.  $diag[\mathbf{a}]$  is a diagonal matrix whose diagonal entries are the elements of the vector  $\mathbf{a}$ .  $\mathbf{W}$  is the normalized  $N \times N$  DFT matrix. The unit impulse function is denote by  $\delta(n)$  which is equal to one when  $n = 0$  and zero otherwise.  $\otimes$  and  $\otimes_c$  denote the linear convolution and circular convolution respectively.

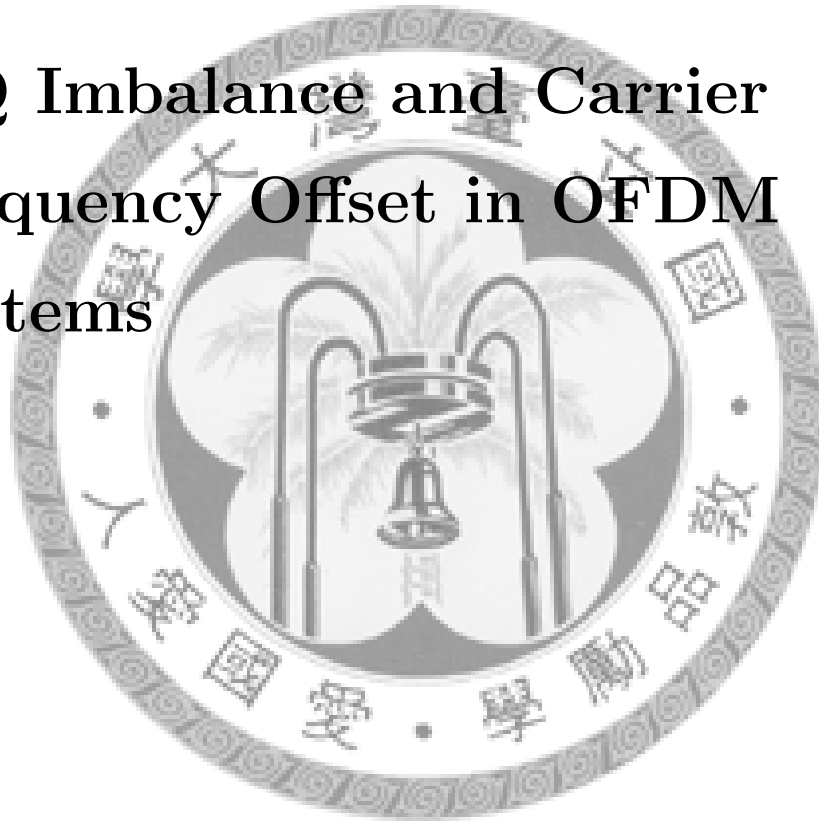






## Chapter 2

# I/Q Imbalance and Carrier Frequency Offset in OFDM Systems



OFDM (orthogonal frequency division multiplexing) is an effective method to provide bandwidth efficiency and to mitigate ISI (inter-symbol interference) in handling time dispersion of multi-path fading channels. However, it is susceptible to the impairments caused by the imperfectness in the RF signal down-conversion process. This leads either to stringent front-end specifications and, thus, an expensive device, or large performance degradations. I/Q imbalance and CFO are known to be the key nonidealities for OFDM receivers.

Although a number of compensation schemes were proposed in the analog domain to calibrate the I/Q branches and the frequency of the local oscillator, they still suffer from different offsets, errors in the measurement feedback loop, and a long calibration process [3]. The required specifications for systems such as IEEE 802.11a can not be simply met by analog domain techniques [3], [4]. An alternative approach is to estimate and compensate such distortions in the digital domain by digital signal processing. There is always a trade-off in the analog domain between power, speed, and area [8], but this consideration does not exist in the digital domain. As can be shown in this thesis, the I/Q imbalance and CFO can be estimated and compensated along with the channel estimation and equalization procedure in the digital domain.

In Sec. 2.1, an OFDM system model is briefly introduced. In Sec. 2.2, we explain the phenomenon of the I/Q imbalance and CFO. In Sec 2.3, we build a general model for the I/Q imbalance and CFO. We discuss the compensation approach in Sec 2.4. The simulation results and comparison are shown in Sec 2.5. Finally some concluding remarks are drawn in Sec. 2.6.

## 2.1 Introduction to OFDM Systems

A block diagram of OFDM system is shown in Fig.2.1. At the transmitter, an  $N \times 1$  data symbol vector  $\mathbf{s}$  consists of modulated data, where  $N$  is the number of subchannels. after taking the  $N$ -point normalized IDFT of the vector  $\mathbf{s}$  is defined as

$$\mathbf{x} = \mathbf{W}^H \mathbf{s} \quad (2.1)$$

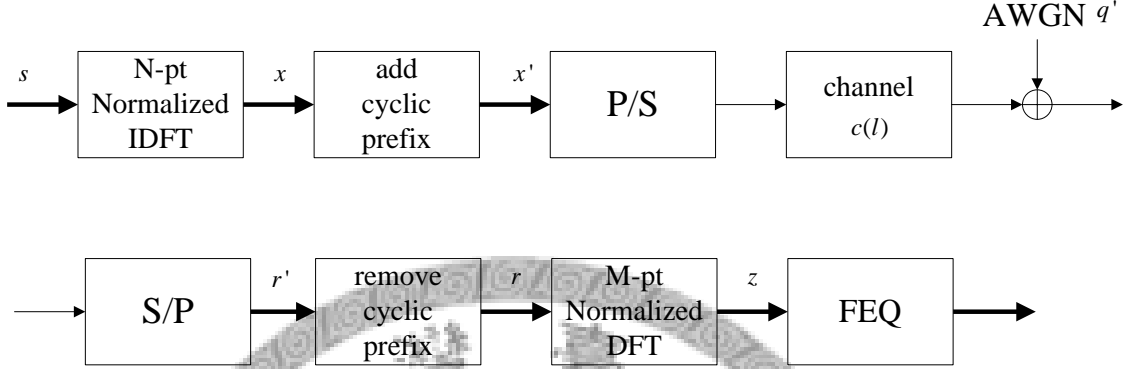


Figure 2.1: Block diagram of OFDM system

where the matrix  $\mathbf{W}$  is defined as

$$[\mathbf{W}]_{m,n} = \frac{1}{\sqrt{N}} e^{-j \frac{2\pi}{N} mn}, \text{ for } m, n = 0, 1, \dots, N-1 \quad (2.2)$$

and

$$\mathbf{W}\mathbf{W}^H = \mathbf{W}^H\mathbf{W} = \mathbf{I}_N \quad (2.3)$$

The next operation of the transmitter is adding cyclic prefix (CP). A CP of length  $L$  that is larger than or equal to the order of the channel is added to  $\mathbf{x}$  in order to eliminate the inter-symbol interference (ISI) caused by multipath propagation. The operation of adding CP to the vector  $\mathbf{x} = [x(0) \ x(1) \ \dots \ x(N-1)]^T$  is

$$\mathbf{x}' = \underbrace{\begin{bmatrix} \mathbf{0}_{L \times (N-L)} & \mathbf{I}_L \\ & \mathbf{I}_N \end{bmatrix}}_{\mathbf{T}_1} \mathbf{x} \quad (2.4)$$

$$= \underbrace{[x(N-L) \ x(N-L+1) \ \dots \ x(0) \ x(1) \ \dots \ x(N-1)]^T}_{\text{CP}} \quad (2.5)$$

The length of the vector  $\mathbf{x}'$  is  $(N+L)$ . The vector  $\mathbf{x}'$  is converted into a sequence by a parallel-to-serial conversion. Then it is transmitted over the channel.

It is assumed that the order of the channel is not larger than the CP length  $L$ , that is,  $c(l) = 0$  for  $l > L$  and  $l < 0$ . Here we assume that the channel is quasi-static. That means that channel is time invariant during a data symbol block transmission. The effect of channel is linear convolution between  $c(l)$  and transmitted signals. The result of linear convolution between  $c(l)$  and transmitted signals can be represented by two  $(N + L) \times (N + L)$  matrices as follows

$$\begin{aligned} \mathbf{r}' &= \mathcal{C}_1 \mathbf{x}' + \mathcal{C}_0 \mathbf{x}'_{prev} + \mathbf{q}' \\ &= \mathcal{C}_1 \mathbf{T}_1 \mathbf{x} + \mathcal{C}_0 \mathbf{T}_1 \mathbf{x}_{prev} + \mathbf{q}' \end{aligned} \quad (2.6)$$

where

$$\mathcal{C}_1 = \begin{bmatrix} c(0) & 0 & \dots & \dots & \dots & 0 \\ \vdots & c(0) & \ddots & & & \vdots \\ c(L) & \vdots & & & & \vdots \\ 0 & c(L) & \ddots & & & \vdots \\ \vdots & \vdots & \ddots & & & 0 \\ 0 & \dots & 0 & c(L) & \dots & c(0) \end{bmatrix} \quad (2.7)$$

and

$$\mathcal{C}_0 = \begin{bmatrix} 0 & \dots & 0 & c(L) & \dots & c(1) \\ \vdots & & & 0 & \ddots & \vdots \\ \vdots & & & & & c(L) \\ \vdots & & & & & 0 \\ \vdots & & & & & \vdots \\ 0 & \dots & \dots & \dots & \dots & 0 \end{bmatrix} \quad (2.8)$$

and  $\mathbf{x}'_{prev}$  denotes the previous transmitted data block. The noise vector  $\mathbf{q}'$  is the blocked version of the channel noise  $q'(n)$ . We assume that the channel noise  $q'(n)$  is zero-mean circularly-symmetric complex additive white Gaussian noise (AWGN).

At the receiver, the received signal is first converted into a vector. After discarding

the  $L$  CP samples, we obtain

$$\begin{aligned} \mathbf{r} &= \underbrace{[\mathbf{0}_{N \times L} \ \mathbf{I}_N]}_{\mathbf{T}_2} \mathbf{r}' \\ &= [r'(L) \ r'(L+1) \ \dots \ r'(N+L-1)]^T \end{aligned} \quad (2.9)$$

From  $\mathbf{T}_1$  in (2.4),  $\mathbf{T}_2$  in (2.9), (2.7), and (2.8), we can find that

$$\mathbf{C} = \mathbf{T}_2 \mathbf{C}_1 \mathbf{T}_1 = \begin{bmatrix} c(0) & 0 & \dots & 0 & c(L) & \dots & c(1) \\ c(1) & c(0) & \dots & \dots & \dots & \dots & \vdots \\ \vdots & \vdots & \dots & \dots & \dots & \dots & c(L) \\ c(L) & \dots & \dots & \dots & \dots & \dots & 0 \\ 0 & \dots & \dots & \dots & \dots & \dots & \vdots \\ \vdots & \vdots & \dots & \dots & \dots & \dots & 0 \\ 0 & \dots & 0 & c(L) & \dots & c(1) & c(0) \end{bmatrix} \quad (2.10)$$

and

$$\mathbf{T}_2 \mathbf{C}_0 = \mathbf{0}_N \quad (2.11)$$

Notice that  $\mathbf{C}$  is an  $N \times N$  circulant matrix and  $\mathbf{C}'$  is an  $N \times N$  zero matrix. Because of CP, linear convolution between the channel and transmitted signals becomes circular convolution. In addition, the interference due to the previous data block (inter-block interference, IBI) is completely eliminated.

Subsequently, the vector  $\mathbf{r}$  is passed through an  $N$ -point normalized discrete Fourier transform (DFT). Then we have

$$\begin{aligned} \mathbf{z} &= \mathbf{W}\mathbf{r} = \mathbf{W}\mathbf{T}_2\mathbf{r}' \\ &= \mathbf{W}\mathbf{T}_2(\mathbf{C}_1\mathbf{T}_1\mathbf{x} + \mathbf{C}_0\mathbf{T}_1\mathbf{x}_{prev} + \mathbf{q}') \\ &= \mathbf{W}\mathbf{C}\mathbf{x} + \mathbf{W}\mathbf{q} \\ &= \mathbf{W}\mathbf{C}\mathbf{W}^H\mathbf{s} + \mathbf{W}\mathbf{q} \end{aligned} \quad (2.12)$$

where  $\mathbf{q} = \mathbf{T}_2\mathbf{q}'$ . It can be shown that

$$\mathbf{W}\mathbf{C}\mathbf{W}^H = \mathbf{D}_\Lambda \quad (2.13)$$

where

$$\mathbf{D}_\Lambda = \text{diag}[C(0), C(1), \dots, C(N-1)] \quad (2.14)$$

and

$$C(k) = \sum_{l=0}^L c(l)e^{-j\frac{2\pi}{N}kl} \quad (2.15)$$

From (2.12) and (2.38), we obtain

$$\mathbf{z} = \mathbf{D}_\Lambda \mathbf{s} + \mathbf{W}\mathbf{q} \quad (2.16)$$

Since  $\mathbf{D}_\Lambda$  is a diagonal matrix, the finite impulse response (FIR) channel is converted into  $N$  frequency-nonsselective parallel subchannels, each subchannel does not suffer from ISI caused by other subchannels.

We can select frequency domain equalizer (FEQ) as one-tap zero forcing (ZF) FEQ, then

$$\mathbf{D}_\Lambda^{-1} = \text{diag} \left[ \frac{1}{C(0)}, \frac{1}{C(1)}, \dots, \frac{1}{C(N-1)} \right] \quad (2.17)$$

Finally, the recovered data symbol vector is

$$\hat{\mathbf{s}} = \mathbf{s} + \mathbf{D}_\Lambda^{-1} \mathbf{W}\mathbf{q} \quad (2.18)$$

Notice that, the OFDM system with ZF FEQ is a perfect reconstruction (PR) system in the absence of channel noise.

## 2.2 The Phenomenon of I/Q Imbalance and CFO

Down-conversion is a fundamental stage in direct-conversion RF receivers. The radio frequency signal is transferred to the zero frequency (baseband) by multiplying a local oscillating signal. The down-conversion from the radio frequency to baseband is implemented as shown in Fig. 2.2. Both in-phase (I) waveforms and quadrature-phase (Q) waveforms are required to perform the complex down-conversion. As seen in Fig. 2.2, the direct-conversion receiver is divided into I branch and Q branch which respectively represent the real and imaginary parts of the equivalent baseband signal.

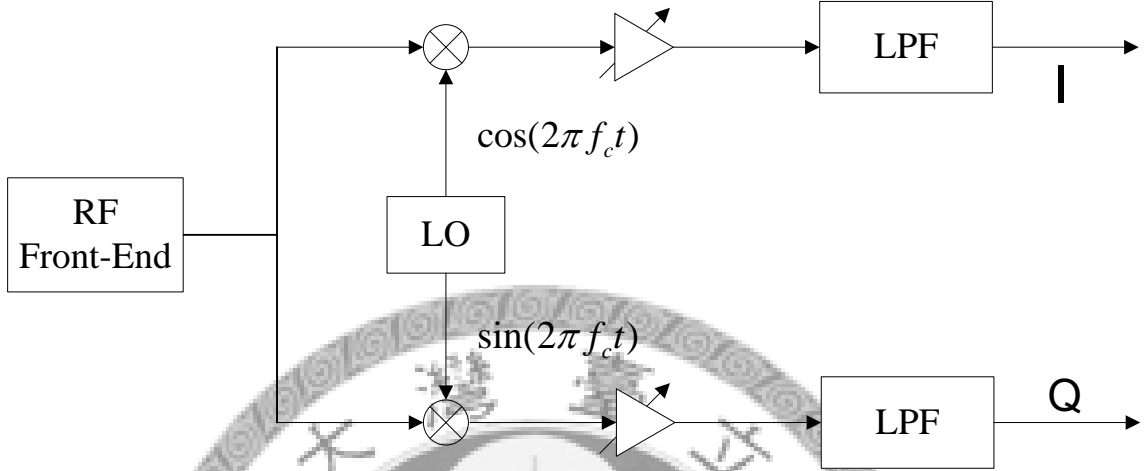


Figure 2.2: Idea direct-conversion receiver

Each branch is followed by amplification, channel select filtering and digitization. The waveforms of I branch and Q branch at the receiver need to be orthogonal, i.e. exactly with  $90^\circ$  difference and with the same amplitude and frequency. The overall I/Q imbalance after down-conversion results from the phase or amplitude mismatches between I branch and Q branch which significantly affects the performance of the system.

For silicon implementation, generating orthogonal waveforms at radio frequencies as high as 5.2 GHz (the band of operation for IEEE 802.11a) is a difficult task. Integrated circuit technologies such as low-cost complementary metal-oxide semiconductor (CMOS) technology have considerable mismatch between components due to fabrication process variations including doping concentration, oxide thickness, mobility, and geometrical sizes over the chip [11]. There are unavoidable errors due to process mismatches and temperature variations in analog circuits. In practice, there are several techniques developed in the analog domain to reduce such mismatches. Component mismatches are diminished by layout techniques or by increasing the physical size of the devices to benefit from the averaging over the area [11]. In addition, different circuit topologies have been used in analog circuit designs that are

more robust to component mismatches.

However, these techniques will increase the device sizes and raise the power consumption in the analog domain. Unfortunately, even if the power consumption is increased, the effects of mismatches can not be completely eliminated due to other reasons. Any process variations in resistors or capacitors, layout parasitic, dynamic fabrication, and temperature variations can limit the achievable match between the I branch and Q branch at high carrier frequencies [3]. Therefore, perfect I/Q matching is impossible in the analog domain, especially when low-cost fabrication technologies are used. A more efficient way is to compensate these mismatches in the digital domain.

### 2.2.1 I/Q Imbalance

One of the major RF impairments is the I/Q imbalance, which refers to the mismatch between In-phase and Quadrature-phase branches from the idea case. At a direct-conversion receiver (DCR), there are two kinds of I/Q imbalance: (i) frequency-independent imbalance which is due to the amplitude and the phase mismatches of the local oscillator; (ii) frequency-dependent imbalance, which is caused by mismatched frequency responses of branch component. Both types of I/Q imbalance introduce destructive image interference and limit the system performance significantly.

### 2.2.2 Carrier Frequency offset

OFDM systems have its drawbacks compared to the other single carrier schemes. Its extreme sensitivity is time varying multiplicative effects such as fading, Doppler shifts and oscillator jitter. Doppler shifts and oscillator jitter result in a mismatch between the carrier frequency of the received signal and the local oscillator (LO). Carrier frequency offset (CFO) is due the the mismatch.



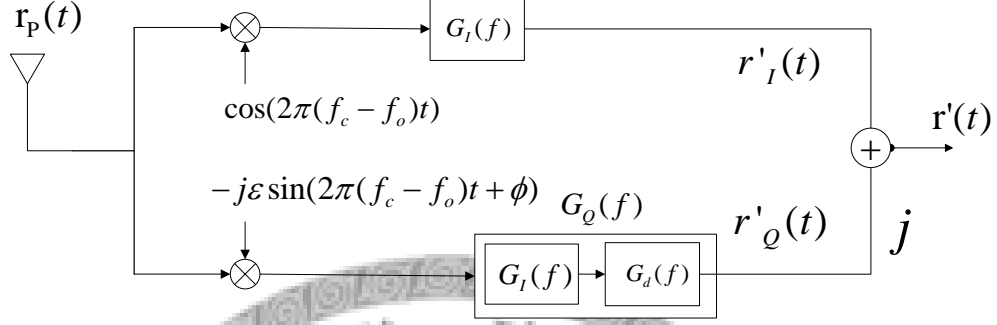


Figure 2.3: Arithmetic model for DCR with I/Q imbalance and CFO

## 2.3 I/Q Imbalance and CFO on the Received Baseband Signal Model

At the receiver, the frequency down-conversion is first used to convert an RF signal into a baseband signal. Fig.2.3 shows the arithmetic model for the frequency down-conversion. The passband signal at the antenna of the receiver is denoted by  $r_p(t)$  and it is given by

$$\begin{aligned} r_p(t) &= 2\text{Re}\{r_b(t)e^{j2\pi f_c t}\} + q(t) \\ &= r_b(t)e^{j2\pi f_c t} + r_b^*(t)e^{-j2\pi f_c t} + q(t) \end{aligned} \quad (2.19)$$

where  $f_c$  is the carrier frequency,  $r_b(t)$  is the baseband equivalent signal and  $q(t)$  is the additive noise.

At the front-end stage of the down-conversion, the passband signal  $r_p(t)$  is multiplied by a local oscillator signal  $Osc(t)$  which is composed of two orthogonal sinusoidal waves. We consider the mismatched local oscillator with the carrier frequency offset  $f_o$  and I/Q mismatches

$$Osc(t) = \cos(2\pi f_c t - 2\pi f_o t) - j\epsilon \sin(2\pi f_c t - 2\pi f_o t + \phi) \quad (2.20)$$

where  $\epsilon$  models the amplitude imbalance between the I and Q branch,  $\phi$  models the phase orthogonality mismatch.

After multiplied by the local oscillator, the consequent signal is passed through two mismatch low-pass filters (with frequency responses of  $G_I(f)$  and  $G_Q(f)$ , respectively) to obtain the baseband equivalent signal

$$\begin{aligned} r'(t) &= LPF\{r_p(t) Osc(t)\} \\ &= [e^{j2\pi f_o t} r_b(t)] \otimes g_+(t) + [e^{-j2\pi f_o t} r_b^*(t)] \otimes g_-(t) \end{aligned} \quad (2.21)$$

where

$$g_+(t) = F^{-1}\{G_+(f)\} = F^{-1}\left\{\frac{G_I(f) + \epsilon e^{-j\phi} G_Q(f)}{2}\right\} \quad (2.22)$$

$$g_-(t) = F^{-1}\{G_-(f)\} = F^{-1}\left\{\frac{G_I(f) - \epsilon e^{j\phi} G_Q(f)}{2}\right\} \quad (2.23)$$

The distorted baseband signal  $r'(t)$  is sampled to get the discrete-time baseband signal  $r'(n) = r'(t)|_{t=nT_s}$ , where  $T_s$  is the sampling period and  $r_b(t)|_{t=nT_s}$  is the desired discrete-time baseband signal. Note the normalized CFO parameter as  $\theta = f_o/\Delta f$ , where  $\Delta f = 1/(NT_s)$ . Therefore the discrete-time received signal as

$$r'(n) = \left[ e^{j\frac{2\pi n\theta}{N}} r_b(n) \right] \otimes g_+(n) + \left[ e^{-j\frac{2\pi n\theta}{N}} r_b^*(n) \right] \otimes g_-(n) \quad (2.24)$$

In the idea case, ie.  $\theta = 0$ ,  $\epsilon = 1$ ,  $\phi = 0$ ,  $g_I(n) = g_Q(n) = \delta(n)$ , the received signal becomes  $r'(n) = r_b(n)$ .

A block diagram of the OFDM system with I/Q imbalance and CFO is shown in Fig.2.4. The channel does not vary with in an OFDM data symbol block transmission, and the discrete-time equivalent channel impulse response is denoted by  $c(n)$ . We assume that the order of  $c(n)$ ,  $g_I(n)$  and  $g_Q(n)$  are  $N_c$ ,  $N_I$  and  $N_Q$  respectively. Using the I channel frequency response as reference, the frequency dependent I/Q imbalance can be modeled by a different term

$$G_d(f) = \frac{G_Q(f)}{G_I(f)} \quad (2.25)$$

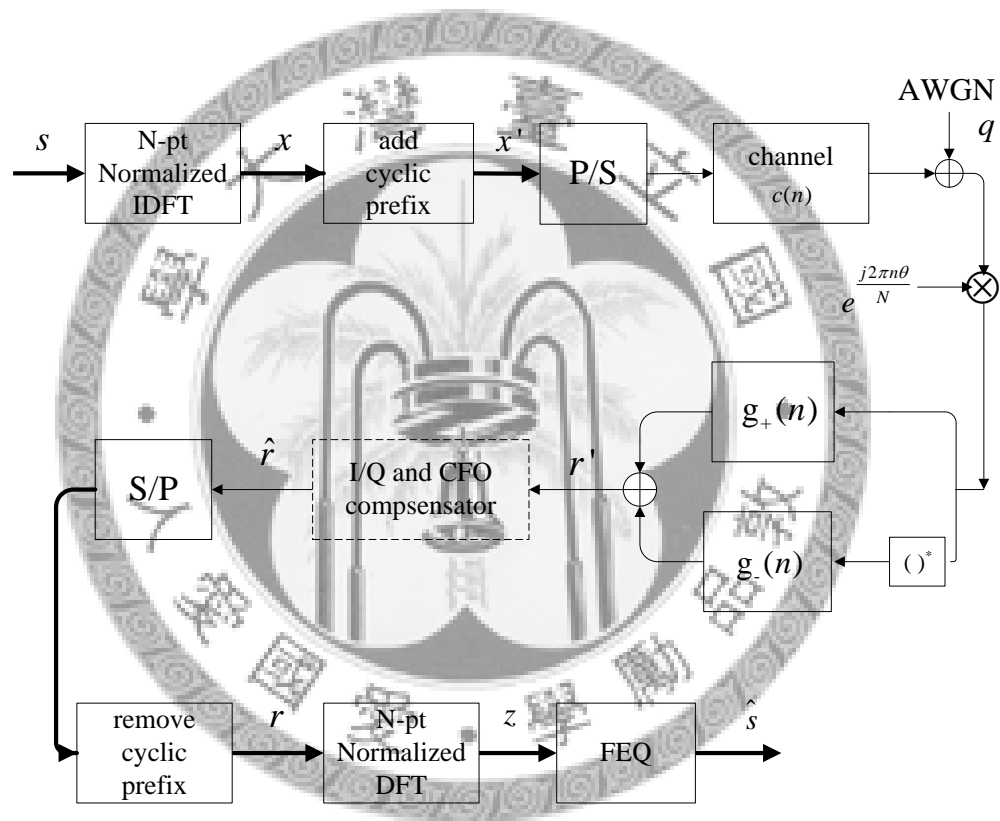


Figure 2.4: A block diagram of OFDM with I/Q imbalance and CFO

where the order of  $g_d(n)$  is defined as  $N_d$ . According to (2.25), (2.24) can rewrite as

$$\begin{aligned} r'(n) &= \left\{ e^{j\frac{2\pi n\theta}{N}} \left[ x(n) \otimes c(n) \otimes \left( e^{-j\frac{2\pi n\theta}{N}} g_I(n) \right) \right] \right\} \otimes \left( \frac{\delta(n) + \epsilon e^{-j\phi} g_d(n)}{2} \right) \\ &+ \left\{ e^{-j\frac{2\pi n\theta}{N}} \left[ x^*(n) \otimes c^*(n) \otimes \left( e^{j\frac{2\pi n\theta}{N}} g_I(n) \right) \right] \right\} \otimes \left( \frac{\delta(n) - \epsilon e^{j\phi} g_d(n)}{2} \right) \\ &+ q'(n) \end{aligned} \quad (2.26)$$

where

$$q'(n) = q(n) \otimes g_+(n) + q^*(n) \otimes g_-(n) \quad (2.27)$$

To simplify (2.26), we define  $h(n) \triangleq c(n) \otimes \left( e^{-j\frac{2\pi n\theta}{N}} g_I(n) \right)$ . The order of  $h(n)$  is  $N_h$ . Therefore, (2.26) becomes

$$\begin{aligned} r'(n) &= \left\{ e^{j\frac{2\pi n\theta}{N}} [x(n) \otimes h(n)] \right\} \otimes \left( \frac{\delta(n) + \epsilon e^{-j\phi} g_d(n)}{2} \right) \\ &+ \left\{ e^{-j\frac{2\pi n\theta}{N}} [x^*(n) \otimes h^*(n)] \right\} \otimes \left( \frac{\delta(n) - \epsilon e^{j\phi} g_d(n)}{2} \right) \\ &+ q'(n) \end{aligned} \quad (2.28)$$

## 2.4 Compensation of I/Q Imbalance and CFO

We have shown the mathematical model of OFDM systems distorted by I/Q compensation and CFO in Section 2.3. Now we illustrate the compensation structure proposed by [12] at the OFDM receiver shown in Fig 2.5. Given the estimates of  $w(n)$ ,  $\alpha$ ,  $\beta$  and  $\hat{\theta}$ , the method of compensating I/Q imbalance and CFO is discussed in this section. As explained in Section 2.1, the I/Q imbalance contains a frequency dependent part and a frequency independent part that will be compensated individually. Since the frequency dependent imbalance attributes to the different LPF responses of analog I/Q branches, it can be coped with digital filters to balance such difference. The compensation for frequency dependent I/Q imbalance can be implemented by inserting an  $N_d$ -order FIR filter  $w(n)$  into the I branch to counteract the mismatched frequency response. After the frequency dependent imbalance has been

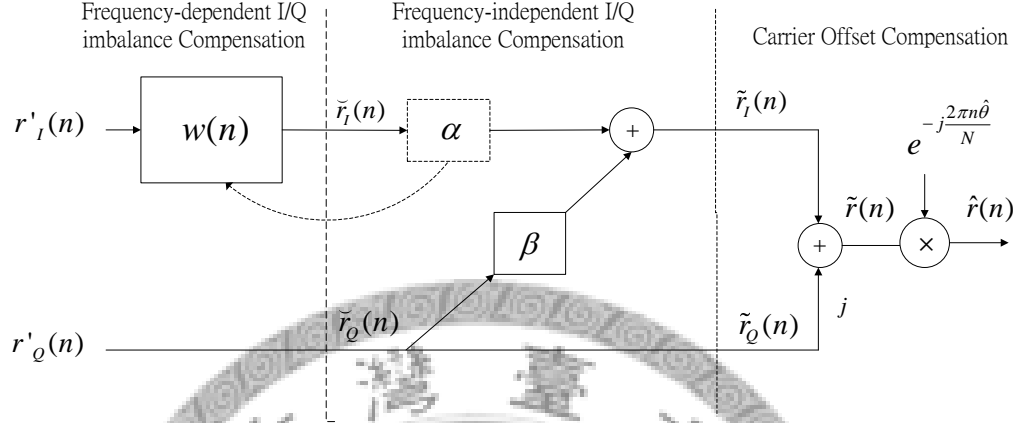


Figure 2.5: compensation structure for I/Q imbalance and CFO proposed in [12]

removed, the remaining frequency independent I/Q imbalance and the carrier offset effect caused by the imbalanced LO can be characterized by a matrix as follows:

$$\begin{bmatrix} \check{r}_I(n) \\ \check{r}_Q(n) \end{bmatrix} = \Phi \begin{bmatrix} \hat{r}_I(n) \\ \hat{r}_Q(n) \end{bmatrix} \quad (2.29)$$

where  $\Phi$  a  $2 \times 2$  matrix defined as

$$\Phi \triangleq \begin{bmatrix} 1 & 0 \\ -\sin \phi & \cos \phi \end{bmatrix} \begin{bmatrix} \cos \frac{2\pi}{N} n\theta & \sin \frac{2\pi}{N} n\theta \\ -\sin \frac{2\pi}{N} n\theta & \cos \frac{2\pi}{N} n\theta \end{bmatrix} \quad (2.30)$$

Hence we compensate CFO and the phase mismatch to recover the ideal baseband signal

$$\begin{bmatrix} \hat{r}_I(n) \\ \hat{r}_Q(n) \end{bmatrix} = \Phi^{-1} \begin{bmatrix} \check{r}_I(n) \\ \check{r}_Q(n) \end{bmatrix} \quad (2.31)$$

Note  $\Phi^{-1}$  can be expressed as

$$\Phi^{-1} = \begin{bmatrix} \cos \frac{2\pi}{N} n\theta & -\sin \frac{2\pi}{N} n\theta \\ \sin \frac{2\pi}{N} n\theta & \cos \frac{2\pi}{N} n\theta \end{bmatrix} \begin{bmatrix} \cos \phi & -\sin \phi \\ \sin \phi & \cos \phi \end{bmatrix} \begin{bmatrix} \frac{1}{\cos \phi} & \tan \phi \\ 0 & 1 \end{bmatrix} \quad (2.32)$$

From the above expression, the gain factor  $\alpha$  and  $\beta$  in Fig. 2.5 correspond to  $\frac{1}{\cos \phi}$  and  $\tan \phi$ , respectively. To further simplify the compensation structure,  $\alpha$  can be merged

into  $w(n)$ , therefore  $w(n)$  is chosen as

$$w(n) = \frac{\epsilon}{\cos \phi} g_d(n) \quad (2.33)$$

Through the compensation structure, the signal can express as

$$\begin{aligned} \hat{r}(n) &= x(n) \otimes c(n) \otimes \left( e^{-j\frac{2\pi n\theta}{N}} g_I(n) \right) \otimes \left( e^{-j\frac{2\pi n\theta}{N}} \epsilon e^{-j\phi} g_d(n) \right) \\ &+ \hat{q}(n) \end{aligned} \quad (2.34)$$

$$= x(n) \otimes h'(n) + \hat{q}(n) \quad (2.35)$$

where the equivalent channel defined as

$$h'(n) \triangleq c(n) \otimes \left( e^{-j\frac{2\pi n\theta}{N}} g_I(n) \right) \otimes \left( e^{-j\frac{2\pi n\theta}{N}} \epsilon e^{-j\phi} g_d(n) \right) \quad (2.36)$$

and

$$\hat{q}(n) = q(n) \otimes h'(n) \quad (2.37)$$

At the receiver, the order of  $h'(n)$  is also equal to  $N_h$  if  $N_I = N_Q$ . We assume the CP length  $L$  is larger than the equivalent channel order and the noise  $\hat{q}(n)$  is assumed as AWGN. As discussed in Sec 2.1, we can rebuild the data signal as

$$\hat{\mathbf{s}} = \mathbf{D}_\Lambda^{-1} \mathbf{z} \quad (2.38)$$

where

$$\mathbf{D}_\Lambda^{-1} = \text{diag} \left[ \frac{1}{H'(0)}, \frac{1}{H'(1)}, \dots, \frac{1}{H'(N-1)} \right] \quad (2.39)$$

and

$$H'(k) = \sum_{n=0}^{N_h} h'(n) e^{-j\frac{2\pi}{N}nk} \quad (2.40)$$

## 2.5 Simulation Result and Comparison

In the following examples, we carry out Monte Carlo experiments to show bit error rate (BER) performance of OFDM systems in the presence of I/Q imbalance and CFO. The channel is supposed to be quasi-static with order  $N_c = 4$  and the length

of CP  $L$  satisfies  $L > N_h - 1$ , so that there are no IBI after CP removal. Channel taps are independent and identically distribution (i.i.d.) complex Gaussian random variables and the variance of the channel taps is normalized by  $\sum_{n=0}^{N_c} \mathbb{E}\{|c(n)|^2\} = 1$ . Assume that the noise is AWGN with noise power  $\mathcal{N}_0$ , and the modulated symbols are QPSK with symbol power  $\mathcal{E}_s$ . The SNR is defined as  $\mathcal{E}_s/\mathcal{N}_0$ . The size of the DFT matrix is  $N = 64$ .

**Example 2.1** In this example, there is no CFO and we only consider the effect of I/Q imbalance in OFDM systems. We consider the I/Q imbalance scenario in [16], where the amplitude and phase mismatches are  $\epsilon = 5dB$  and  $\phi = 5^\circ$ . The LPF of I-branch and Q-branch are  $\mathbf{g}_I = [1 \ 0.1]^T$  and  $\mathbf{g}_Q = [1 \ -0.1]^T$  respectively. As the result, the ideal  $g_d(n)$  is IIR filter. We assume that  $w(n)$  has 5 taps ( $N_d = 5$ ) for containing 98% of energy. The optimum values of the filter is  $\mathbf{w}_{opt} = [w_{opt}(0) \ w_{opt}(1) \ \dots \ w_{opt}(N_d - 1)]^T = \frac{\epsilon}{\cos\phi} [1 \ -0.2 \ 0.02 \ -0.002 \ 0.0002]^T$ . The CP length is 5 to avoid IBI. Notice perfect compensation means that  $w(n)$  and  $c(n)$  are known at the receiver, and I/Q imbalance is compensated perfectly. Furthermore, no compensation means that the receiver do not have the compensation structure in Fig.2.4.

Fig. 2.6 show the comparison of an perfect I/Q imbalance compensation receiver and a receiver without I/Q imbalance compensation. The degradation cause by I/Q imbalance is significant, and the BER curve floors at  $3 \times 10^{-4}$  due to I/Q imbalance. The performance of I/Q distorted receiver does not depend on SNR in the high SNR region. Therefore, the performance of OFDM systems is dominated by I/Q imbalance at high SNR, and this phenomenon reveals that the important role of I/Q imbalance compensation.

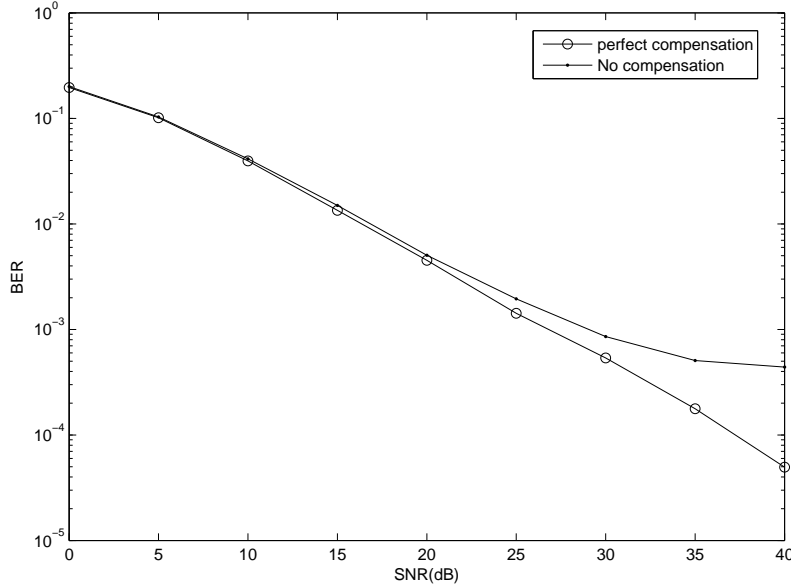


Figure 2.6: Example 2.1. Effect of I/Q imbalance on BER performance of OFDM systems

**Example 2.2** In this example, suppose that there is no I/Q imbalance and we only consider the effect of CFO in OFDM systems. Suppose that SNR is 30dB. Notice that the case: perfect compensation means that  $\theta$  and  $c(n)$  are known at the receiver, therefore, CFO is compensated perfectly. No compensation means that the receiver do not have the compensation structure in Fig.2.4.

The BER performance of OFDM systems versus the normalized CFO parameter is shown in Fig.2.7. We can find that the BER curve increases severely when the normalized is about 0 to 0.2. In other words, the small CFO will destroy the orthogonality seriously in OFDM systems due to ICI caused by CFO. It is found that without proper CFO compensation, OFDM systems suffer a serious performance loss. With the compensation scheme, the BER performance can be significantly improved.



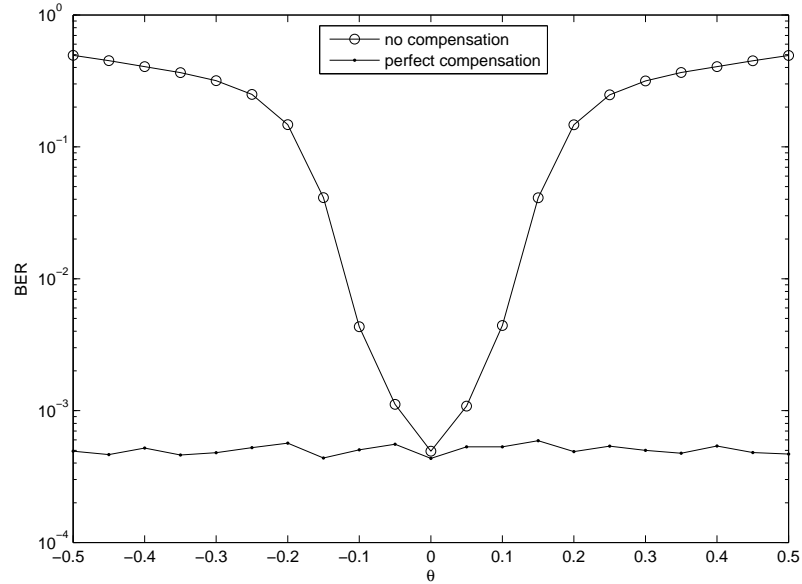


Figure 2.7: Example 2.2. Effect of CFO on BER performance of OFDM systems

**Example 2.3** Joint I/Q imbalance and CFO effect is considered in this example. The actual I/Q imbalance are the same as example 2.1. The CFO parameter  $\theta = 0.2$ . Notice that the case: perfect compensation means that  $w(n)$ ,  $c(n)$  and  $\theta$  are known at the receiver, and I/Q imbalance is compensated perfectly. Furthermore, no compensation means that the receiver do not have the compensation structure in Fig.2.4.

We can see that the comparison of an ideal OFDM receiver and a receiver without I/Q imbalance and CFO compensation in Fig.2.8. OFDM systems can not work if we do not estimate and compensate I/Q imbalance and CFO. Therefore, it is important to estimate and compensate the I/Q imbalance and CFO.

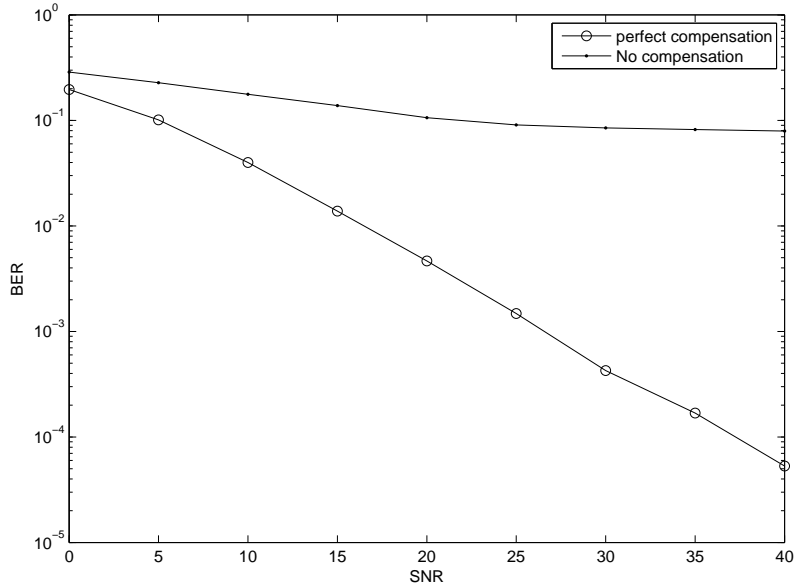


Figure 2.8: Example 2.3. Joint effect of CFO and I/Q imbalance on BER performance of OFDM systems

## 2.6 Concluding Remark

In this chapter, we derived the signal model with I/Q imbalance and CFO mismatch. We also investigated the effect of the I/Q imbalance and CFO in OFDM systems. We showed how to recover the transmitted symbols when the mismatch parameters are known at the receiver. In the simulation, we see that the BER performance of OFDM systems is very bad without proper compensation. With the compensation method, the BER performance can be significantly improved.

## Chapter 3

# Estimation and Compensation of CFO and I/Q imbalance



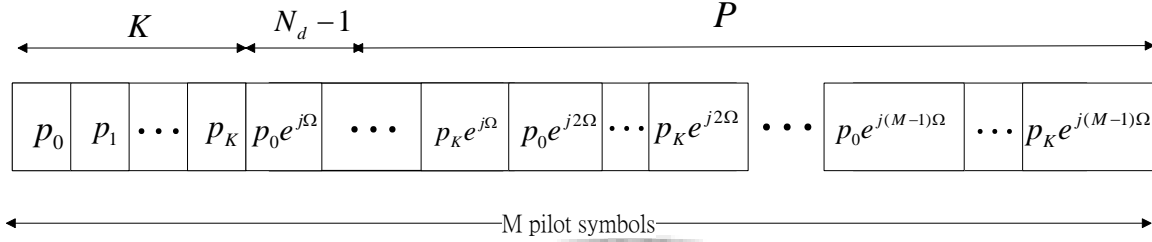


Figure 3.1: Generalized periodic pilot

In the previous chapter, we described the model of I/Q imbalance and CFO, and formulated the influence on the received signals. Then we studied the impacts of I/Q imbalance and CFO on OFDM systems. We introduced a compensation scheme based on the estimated parameters to recover the correct signals. If we can perfectly estimate these unknown parameters ( $\theta$ ,  $w(n)$ , and  $\phi$ ) from certain methods, we can remove these non-idealities.

In this chapter, we will concentrate on how to estimate all the parameters of non-idealities in the time domain, including  $\theta$ ,  $g_d(n)$ ,  $\epsilon$ , and  $\Phi$  discussed in chapter 2. In Sec. 3.1, we review the GPP method in [13]. In Sec. 3.2, we review the CFO estimation in the presence of the I/Q imbalance by using three blocks[14]. We have some simulation results in Sec.3.3. Finally some concluding remarks are drawn in Sec. 3.4.

### 3.1 Pilot Aided Compensation for CFO and I/Q Imbalance by GPP method

In order to accurately estimation the unknown parameters, we introduce *Generalized Periodic Pilot* (GPP) method [13] shown in Fig. 3.1. The GPP consists of M identical symbols where each symbol consists of K samples. However, between two adjacent pilot symbols, there is only one common phase difference  $\Omega$ .

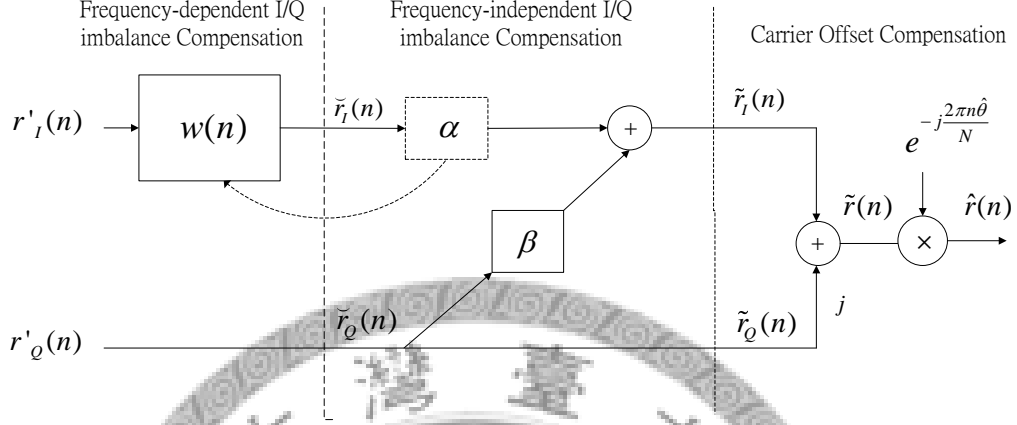


Figure 3.2: compensation structure for I/Q imbalance and CFO

Recall Fig.3.2, the signal after the I/Q imbalance compensation is defined as  $\tilde{r}(n)$ . Suppose that  $K \geq N_h - 1$ , so that the first symbol can be treated as the CP for the whole pilot sequence. To simplify the problem, we discard the first  $(K + N_d - 1)$  samples of  $\tilde{r}(n)$ , where  $K$  samples for the CP and  $N_d$  is the order of  $w(n)$ . Define  $n_0 = K + N_d - 1$  and  $P = MK - n_0$ . After discarding  $n_0$  samples of  $\tilde{r}(n)$ , we collect the remaining  $P$  samples of  $\tilde{r}(n)$ ,  $n_0 \leq n \leq MK - 1$ . Arrange those  $P$  samples in two  $(P - K) \times 1$  sub-vectors. That is

$$\tilde{\mathbf{r}}_1 = [\tilde{r}(n_0) \cdots \tilde{r}(n_0 + P - K - 1)]^T \quad (3.1)$$

$$\tilde{\mathbf{r}}_2 = [\tilde{r}(n_0 + K) \cdots \tilde{r}(n_0 + P - 1)]^T \quad (3.2)$$

Notice that when the I/Q imbalance is perfectly compensated we have

$$\tilde{r}(n + K) = e^{j(\eta + \Omega)} \tilde{r}(n) \quad (3.3)$$

where  $\eta = \frac{2\pi K\theta}{N}$ .

Next we will express  $\tilde{\mathbf{r}}_1$  and  $\tilde{\mathbf{r}}_2$  in the terms of  $r'_I(n)$ ,  $r'_Q(n)$ ,  $w(n)$  and  $\beta$ . Define the vector  $\mathbf{r}_{1,Q} \triangleq [r'_Q(n_0) \cdots r'_Q(n_0 + P - K - 1)]^T$ , and the  $(P - K) \times N_d$  matrix  $\mathbf{R}_{1,I}$  with the  $(i, j)$ th entry given by  $r'_I(n_0 + i - j)$ , where  $r'_I(n)$  and  $r'_Q(n)$  are the real

part and the imaginary of  $r'(n)$ . Then we can write the vector  $\tilde{\mathbf{r}}_1$  as

$$\tilde{\mathbf{r}}_1 = (\mathbf{R}_{1,I}\mathbf{w} + \beta\mathbf{r}_{1,Q}) + j\mathbf{r}_{1,Q} \quad (3.4)$$

where  $\mathbf{w} = [w(0) w(1) w(N_d - 1)]$ . Similarly, by replacing  $n$  by  $(n + K)$ , we can also write

$$\tilde{\mathbf{r}}_2 = (\mathbf{R}_{2,I}\mathbf{w} + \beta\mathbf{r}_{2,Q}) + j\mathbf{r}_{2,Q} \quad (3.5)$$

Apparently, with no noise and perfect I/Q compensation, the  $\tilde{\mathbf{r}}_1$  and  $\tilde{\mathbf{r}}_2$  match the relation given by (3.3), we can write  $\tilde{\mathbf{r}}_2 = e^{j(\eta+\Omega)}\tilde{\mathbf{r}}_1$ . Hence, finding the optimal  $\theta$ ,  $\beta$  and  $\mathbf{w}$  that minimize

$$\left(\hat{\theta}, \hat{\beta}, \hat{\mathbf{w}}\right) = \arg \min_{\theta, \beta, \mathbf{w}} \|\tilde{\mathbf{r}}_2 - e^{j(\eta+\Omega)}\tilde{\mathbf{r}}_1\|^2 \quad (3.6)$$

Substituting (3.4) and (3.5) into (3.6), we find that the cost function is minimized when

$$\begin{cases} \mathbf{r}_{1,Q} \cos(\eta + \Omega) + \mathbf{R}_{1,I}\mathbf{w} \sin(\eta + \Omega) + \beta\mathbf{r}_{1,Q} \sin(\eta + \Omega) = \mathbf{r}_{2,Q} \\ -\mathbf{r}_{1,Q} \sin(\eta + \Omega) + \mathbf{R}_{1,I}\mathbf{w} \cos(\eta + \Omega) + \beta\mathbf{r}_{1,Q} \cos(\eta + \Omega) = \mathbf{R}_{2,I}\mathbf{w} + \beta\mathbf{r}_{2,Q} \end{cases} \quad (3.7)$$

Actually, we can write the above equations in matrix form.

$$[\mathbf{r}_{1,Q} \ \mathbf{R}_{1,I}] \begin{bmatrix} \cos(\eta + \Omega) + \beta \sin(\eta + \Omega) \\ \mathbf{w} \sin(\eta + \Omega) \end{bmatrix} = \mathbf{r}_{2,Q} \quad (3.8)$$

Furthermore, we can also write

$$[\mathbf{r}_{2,Q} \ -\mathbf{R}_{2,I}] \begin{bmatrix} \cos(\eta + \Omega) - \beta \sin(\eta + \Omega) \\ \mathbf{w} \sin(\eta + \Omega) \end{bmatrix} = \mathbf{r}_{1,Q} \quad (3.9)$$

Combining (3.8) and (3.9), we have

$$\mathbf{\Lambda} \underbrace{\begin{bmatrix} \cos(\eta + \Omega) + \beta \sin(\eta + \Omega) \\ \cos(\eta + \Omega) - \beta \sin(\eta + \Omega) \\ \mathbf{w} \sin(\eta + \Omega) \end{bmatrix}}_{\mathbf{q}} = \begin{bmatrix} \mathbf{r}_{2,Q} \\ \mathbf{r}_{1,Q} \end{bmatrix} \quad (3.10)$$

where

$$\mathbf{\Lambda} = \begin{bmatrix} \mathbf{r}_{1,Q} & \mathbf{0} & \mathbf{R}_{1,I} \\ \mathbf{0} & \mathbf{r}_{2,Q} & -\mathbf{R}_{2,I} \end{bmatrix} \quad (3.11)$$

and  $\mathbf{0}$  is a  $(\hat{P} \times 1)$  zero vector. Define a vector  $\mathbf{q} = [q(0) \ q(1) \ \cdots \ q(N_d + 1)]^T$ . When  $P \geq K + N_d + 2$ ,  $\mathbf{\Lambda}$  is a tall matrix. Therefore, a least-squares estimate of  $\mathbf{q}$  is given by

$$\hat{\mathbf{q}} = \mathbf{\Lambda}^\dagger \begin{bmatrix} \mathbf{r}_{2,Q} \\ \mathbf{r}_{1,Q} \end{bmatrix} \quad (3.12)$$

where  $\mathbf{\Lambda}^\dagger$  is the pseudo-inverse of  $\mathbf{\Lambda}$ . Finally, we obtain a closed-form solution for CFO estimation:

$$\hat{\theta} = \frac{N}{2\pi K} \left\{ \arccos\left(\frac{q(0) + q(1)}{2}\right) - \Omega \right\} \quad (3.13)$$

The coefficients for I/Q imbalance compensation are given by

$$\hat{\beta} = \frac{q(0) - q(1)}{2 \sin(2\pi\hat{\theta}K/N + \Omega)} \quad (3.14)$$

$$\hat{\mathbf{w}} = \frac{1}{\sin(2\pi\hat{\theta}K/N + \Omega)} [q(2) \ q(3) \ \cdots \ q(N_d + 1)]^T \quad (3.15)$$

Consequently, the coefficients can be obtained by simply constructing  $\mathbf{\Lambda}$ ,  $\mathbf{r}_{2,I}$  and  $\mathbf{r}_{1,I}$  from the received pilot symbols, and solving an LLS problem. It is worth noting that only the signals at the I branch are compensated for, while those at the Q branch are just time-shifted and thus can be used as references.

However, the GPP method has three problems. First, while  $\sin(\eta + \Omega) = 0$ , the GPP method cannot estimate the compensation filter  $w(n)$ . Second, because of using cosine function, the performance of the CFO estimation becomes worse when  $(\eta + \Omega) \approx 0$  or  $\pm\pi$ . Third, Letting  $\Omega = \pi/2$ , the CFO estimation range is  $\theta \in (\frac{-N}{4K}, \frac{N}{4K})$ , where  $N$  is the OFDM block size and  $K$  is the length of one pilot symbol.

## 3.2 CFO Estimation by Three-Block method

In the previous section,  $\theta$ ,  $\beta$  and  $\mathbf{w}$  are estimated at the same time. In this section, we review the CFO estimation in the presence of the I/Q imbalance by using

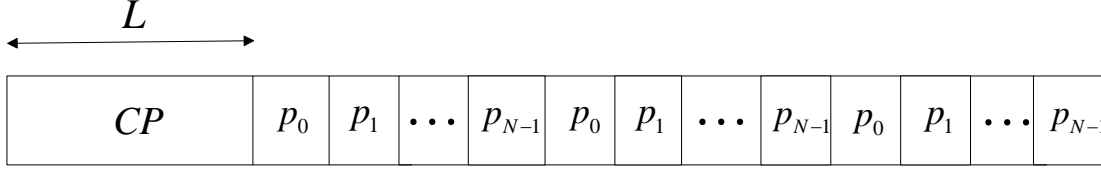


Figure 3.3: Training sequences of Three-Block method

three repeated OFDM blocks[14]. [14] only discusses the frequency independent I/Q imbalance (i.e.,  $g_I(n) = g_Q(n)$ ). But the CFO estimation method in [14] can be applied of frequency dependent I/Q imbalance. Therefore, we only introduce the CFO estimation method.

The training sequences are shown in Fig. 3.3, which consist three identical OFDM blocks. According to (2.28), we rewrite the received signal as

$$r'(n) = \Re\{e^{j\frac{2\pi n\theta}{N}}[x(n) \otimes h(n)]\} + j\Im\{e^{j\frac{2\pi n\theta}{N}}[x(n) \otimes h(n) \otimes g'_d(n)]\} \quad (3.16)$$

where  $g'_d(n) = \epsilon e^{j(\phi - \frac{2\pi n\theta}{N})} g_d(n)$  Assuming CP length  $L$  is large enough, therefore, after remove the CP we have

$$r_I(n + KN) = \Re\{e^{j2K\pi\theta} e^{j\frac{2\pi n\theta}{N}} [x(n) \otimes_c h(n)]\} \quad (3.17)$$

$$r_Q(n + KN) = \Im\{e^{j2K\pi\theta} e^{j\frac{2\pi n\theta}{N}} [x(n) \otimes_c h(n) \otimes_c g'_d(n)]\} \quad (3.18)$$

where  $K = 0, 1, 2$ . Now we define  $r_I(n) = a_n \cos(b_n)$ , where  $a_n$  and  $b_n$  are the magnitude and phase of  $e^{j\frac{2\pi n\theta}{N}} [x(n) \otimes_c h(n)]$  respectively. According to (3.17) we have

$$\begin{aligned} r_I(n + 2N) + r_I(n) &= a_n \cos(b_n + 4\pi\theta) + a_n \cos(b_n) \\ &= 2a_n(\cos(b_n + 2\pi\theta)\cos(2\pi\theta)) \\ &= 2\cos(2\pi\theta)r_I(n + N) \end{aligned} \quad (3.19)$$

Then  $\cos(2\pi\theta)$  can be estimated by

$$\widehat{\cos 2\pi\theta} = \frac{r_I(n + 2N) + r_I(n)}{2r_I(n + N)} \quad (3.20)$$



There exists the same property of the  $r_Q(n)$ , that is

$$\widehat{\cos 2\pi\theta} = \frac{r_Q(n+2N) + r_Q(n)}{2r_Q(n+N)} \quad (3.21)$$

Therefore, the real and imaginary components of the received signal can be used to estimate the CFO. In order to have smaller error variance, both components will be used. Using the LS, the CFO estimate is given by

$$\widehat{\cos 2\pi\theta} = \mathbf{u}^\dagger \mathbf{v} \quad (3.22)$$

where  $\mathbf{u}^\dagger$  denotes the pseudo-inverse of  $\mathbf{u}$  and

$$\mathbf{u} = 2 \begin{bmatrix} r_I(N) \\ r_I(N+1) \\ \vdots \\ r_I(2N-1) \\ r_Q(N) \\ r_Q(N+1) \\ \vdots \\ r_Q(2N-1) \end{bmatrix} \quad (3.23)$$

and

$$\mathbf{v} = \begin{bmatrix} r_I(0) + r_I(2N) \\ r_I(1) + r_I(2N+1) \\ \vdots \\ r_I(N-1) + r_I(3N-1) \\ r_Q(0) + r_Q(2N) \\ r_Q(1) + r_Q(2N+1) \\ \vdots \\ r_Q(N-1) + r_Q(3N-1) \end{bmatrix} \quad (3.24)$$

Then

$$\hat{\theta} = \frac{1}{2\pi} \arccos(\mathbf{u}^\dagger \mathbf{v}) \quad (3.25)$$

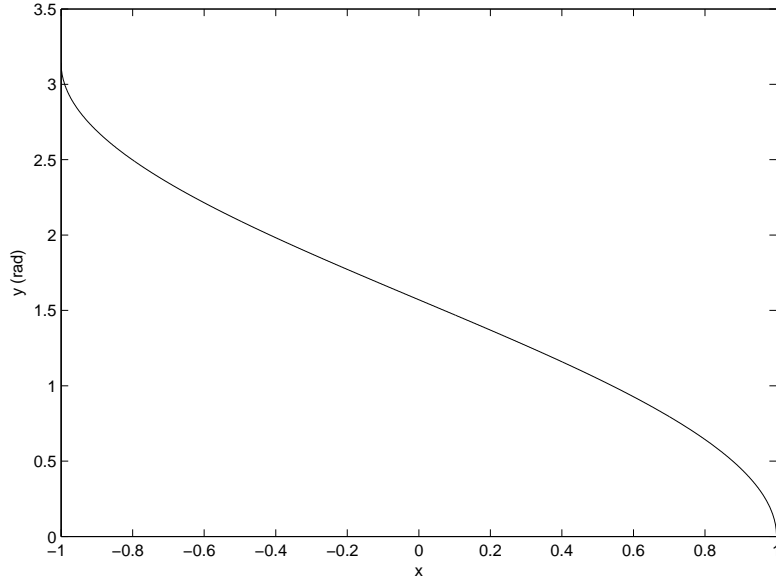


Figure 3.4:  $y = \arccos(x)$

Note that the LLS operation in this instance can be implemented by two dot product operations which have very low computational complexity.

However, there are two problems with this estimator though it is robust to I/Q mismatch. One is the polarity ambiguity problem due to the range of arccos function is  $[0, \pi]$ , the range for  $\theta$  in the estimator needs to be limited to  $[0, \pi/2]$ . The other is, when  $\theta \approx 0$  or  $\theta \approx \pi/2$ , the estimation error of  $\theta$  increases rapidly even that the estimation error of  $\cos 2\pi\theta$  is varying slightly. This is because the gradient of the function  $y = \arccos(x)$  is large when  $x \approx 1$  or  $-1$  as shown in Fig.3.4.

### 3.3 Simulation Results

In this section, we carry out Monte Carlo experiments to show the performance of the estimation methods which introduced in this chapter. The channel is supposed

to be quasi-static with order  $N_c = 4$  and the length of CP  $L$  satisfies  $L > N_h - 1$ , so that there are no IBI after CP removal. Channel taps are independent and identically distribution (i.i.d.) complex Gaussian random variables and the variance of the channel taps is normalized by  $\sum_{n=0}^{N_c} \mathbb{E}\{|c(n)|^2\} = 1$ . Assume that the noise is AWGN with noise power  $\mathcal{N}_0$ , and the modulated symbols are QPSK with symbol power  $\mathcal{E}_s$ . The SNR is defined as  $\mathcal{E}_s/\mathcal{N}_0$ . The size of the DFT matrix is  $N = 64$ . We consider the I/Q imbalance scenario in [16], where the amplitude and phase mismatches are  $\epsilon = 5dB$  and  $\phi = 5^\circ$ . The LPF of I-branch and Q-branch are  $\mathbf{g}_I = [1 \ 0.1]^T$  and  $\mathbf{g}_Q = [1 \ -0.1]^T$  respectively. As the result, the ideal  $g_d(n)$  is IIR filter. We assume that  $w(n)$  has 5 taps ( $N_d = 5$ ) for containing 98% of energy. The estimation MSE is defined as

$$MSE(\theta) = \frac{1}{K} \sum_{i=1}^K |\hat{\theta}^{(i)} - \theta|^2 \quad (3.26)$$

$$MSE(\beta) = \frac{1}{K} \sum_{i=1}^K |\hat{\beta}^{(i)} - \beta|^2 \quad (3.27)$$

$$MSE(\mathbf{w}) = \frac{1}{K} \sum_{i=1}^K \|\hat{\mathbf{w}}^{(i)} - \mathbf{w}\|^2 \quad (3.28)$$

where  $\hat{\theta}$ ,  $\hat{\beta}$  and  $\hat{\mathbf{w}}$  represent the estimated  $\theta$ ,  $\beta$  and  $\mathbf{w}$  respectively.  $\hat{\theta}^{(i)}$ ,  $\hat{\beta}^{(i)}$  and  $\hat{\mathbf{w}}^{(i)}$  stand for the estimated value in  $i$ th trial.  $K = 2000$  denotes the total number of Monte Carlo trials.

**Example 3.1** In this example, we show the performance of the GPP method [12] in Sec3.1. Consider the wireless LAN system of *IEEE802.11a* with carrier frequency 5.2GHz,  $N = 64$  subcarriers, and bandwidth 20MHz. The GPP is generated by adding phase rotate to the short preamble of this system, which corresponds to  $M = 10$  and  $K = 16$ . The phase difference  $\Omega$  is set to  $\pi/2$  as in [13]. The SNR is defined by the ratio of the power of GPP and the variance of channel noise. The GPP method employs  $P = K(M - 2) = 128$ .

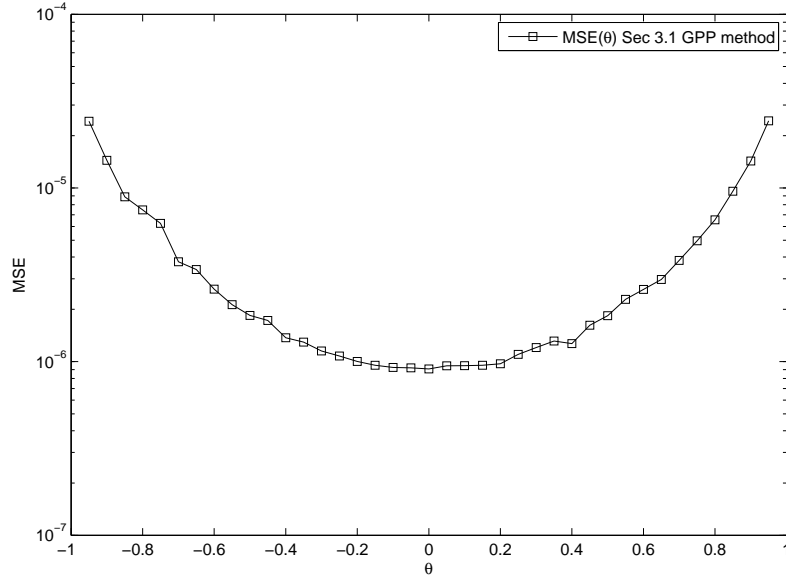


Figure 3.5: Example 3.1. MSE for the estimation of  $\theta$  versus different CFO parameter

Figure 3.5 shows the performance for MSE of estimated CFO versus different value of  $\theta$ . The constant SNR is 30dB. We can see that performance of  $MSE(\theta)$  is worse as the magnitude of  $\theta$  increased. The reason is that CFO estimator use arccos function, which cause the performance fails when  $\theta$  closed to zero. In this example, there are phase shift  $\Omega$ , that implies it rotates the bad performance point from zero to  $\Omega$ .

Figure 3.6 shows the performance for MSE of estimated I/Q imbalance versus different value of  $\theta$ . The constant SNR is also 30dB. We can see that performance of  $MSE(\beta)$  is worse as the magnitude of  $\theta$  increased. Because we have to divide  $\sin(2\pi\theta + \Omega)$  in I/Q estimator. The performance will be significantly effected by the noise, when the value of  $\sin(2\pi\theta + \Omega)$  is very small.

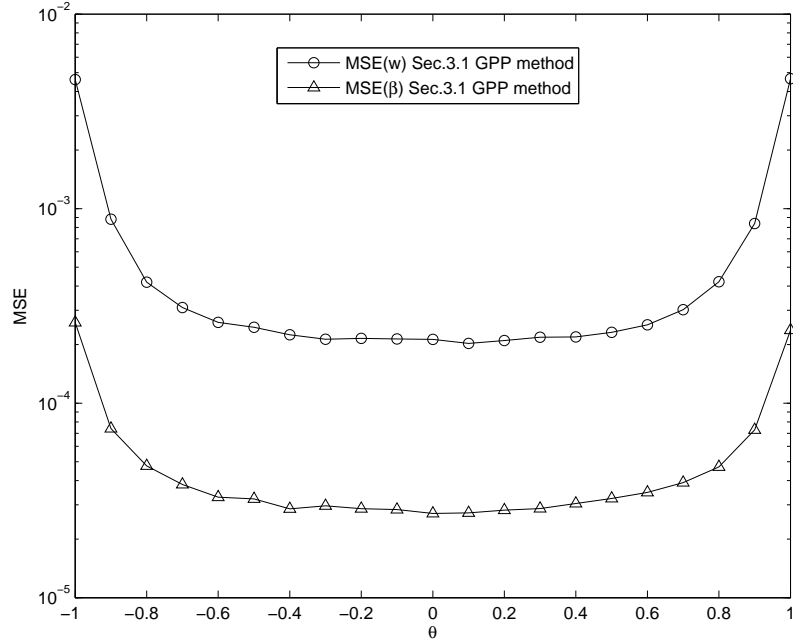


Figure 3.6: Example 3.1. MSE for the estimation of compensation parameter versus different CFO parameter

**Example 3.2** In this example, we show the performance of the CFO estimation method in Section 3.2. We have two identical OFDM blocks of preamble in the system. The OFDM block size  $N = 64$ . Suppose that there are joint influence of I/Q imbalance and CFO.

Figure 3.7 shows the performance for MSE of estimated CFO versus different value of  $\theta$ . The constant SNR is 30dB. We can see that performance of  $MSE(\theta)$  is worse as  $\theta$  approaches 0 and 0.5. The reason is that CFO estimator use arcos function. The disadvantages of using arcos function have been described in section 3.2.

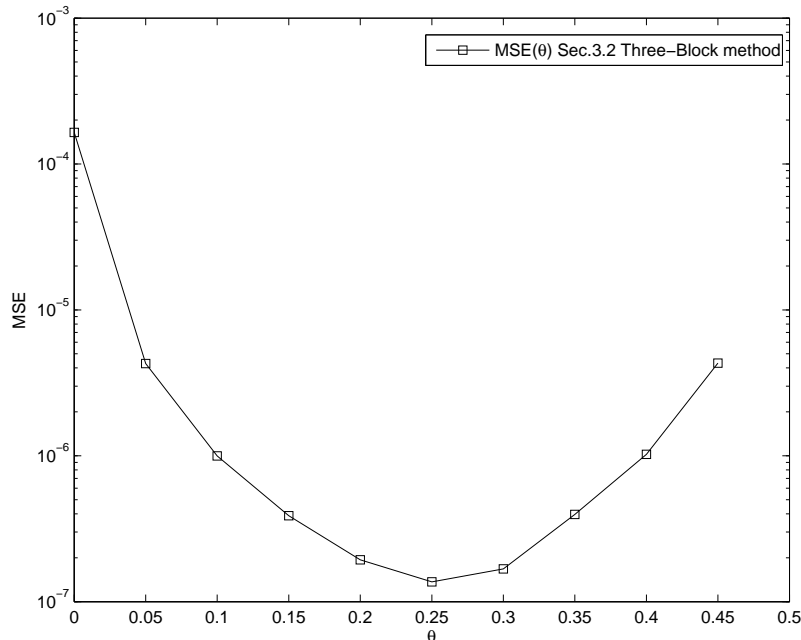


Figure 3.7: Example 3.2. MSE for the estimation of  $\theta$  versus different CFO parameter

### 3.4 Concluding Remark

In this chapter, we review the estimation methods of CFO and I/Q imbalance and discuss the disadvantages at the end of each section. We can estimate  $\theta$ ,  $\mathbf{w}$  and  $\beta$  at the same time as GPP method in Sec 3.1. Or we can estimate  $\theta$  at the first step and then estimate  $\mathbf{w}$  and  $\beta$  by the other methods [12].

In hardware implementation, there is also an issue of latency when CFO is first computed and used to estimate the compensating filter. This is because I/Q imbalance estimation step needs to wait for the CFO value before forming its own LLS matrix. This can be prevented by pre-computing the I/Q imbalance LLS matrix while treating the CFO as variables. After the CFO value is computed, it can be plugged in to the pre-computed matrix hence eliminating the latency.

## Chapter 4

# Joint Estimation of I/Q Imbalance and CFO for OFDM system



In the previous chapter, some estimation algorithms have been given. However, the GPP method has three problems. First, while the  $\sin(\eta + \Omega) = 0$ , the GPP method cannot estimate the compensation filter  $w(n)$ . Second, because of using cosine function, the performance of the CFO estimation becomes worse when  $(\eta + \Omega) \approx 0$  or  $\pm\pi$ . Third, the estimation range is limited in a range of  $(\frac{-N}{4K}, \frac{N}{4K})$  because of the arccos function. The Three-Block method have two problems. First, the performance of CFO estimation becomes worse when  $\theta \approx 0$  or  $0.5$ . And the estimated  $\theta$  of Three-Block method limit to a range of  $(0, 0.5)$ , too.

In this Chapter, we propose a joint estimation method of I/Q imbalance and CFO in Sec 4.1. The proposed method can solve all the problems described above. In Section 4.2, we improve the GPP method, so that the performance of MSE of CFO is still good when  $\theta$  close to  $\Omega$ . We extent the estimation reange of  $\theta$  to  $\theta \in (\frac{-N}{2K}, \frac{N}{2K})$ . In Section 4.3, we improve the Three-block method. We replace the arccos function to the arctan function in the CFO estimator. So that the performance of MSE of CFO is still good when  $\theta$  close to zero or  $0.5$ . Similarly, the estimation range of  $\theta$  extents to  $\theta \in (-0.5, 0.5)$ . The simulation results and comparison are shown in Section 4.4. Finally some concluding remarks are drawn in Sec. 4.5.

## 4.1 Proposed Joint Estimation Method of CFO and I/Q Imbalance

In this section, we consider the presence of the CFO and I/Q Imbalance. The training sequence of the proposed method shown in Fig. 4.1. The proposed method needs two identical OFDM blocks for the preamble. In the proposed method, we estimate  $\theta$  at the first step and the I/Q imbalance parameters at the second step.



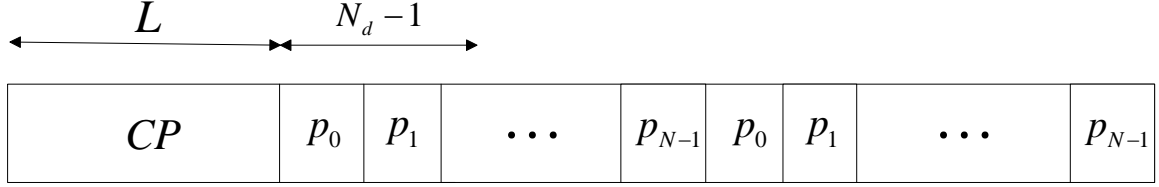


Figure 4.1: Training sequence of proposed method

#### 4.1.1 CFO Estimation

Assume that CP length is large enough so that there is no IBI after removing the CP. The signal after the CP removed is given by  $r(n)$ . Define two  $(N - N_d + 1) \times 1$  vectors

$$\mathbf{r}_{1,I} = [r_I(N_d - 1) \cdots r_I(N - 1)]^T \quad (4.1)$$

$$\mathbf{r}_{1,Q} = [r_Q(N_d - 1) \cdots r_Q(N - 1)]^T \quad (4.2)$$

and an  $(N - N_d + 1) \times N_d$  matrix

$$\mathbf{R}_{1,I} = \begin{bmatrix} r_I(N_d - 1) & r_I(N_d - 2) & \cdots & r_I(0) \\ r_I(N_d) & r_I(N_d - 1) & \cdots & r_I(1) \\ \vdots & \vdots & \ddots & \vdots \\ r_I(N - 1) & r_I(N - 2) & \cdots & r_I(N - N_d) \end{bmatrix} \quad (4.3)$$

where  $r_I(n)$  and  $r_Q(n)$  are the real part and imaginary part of  $r(n)$  respectively. Similarly, the first block can be treated as the CP of the second block. Therefore, we define  $\mathbf{r}_{2,I} = [r_I(N + N_d - 1) \cdots r_I(2N - 1)]^T$ ,  $\mathbf{r}_{2,Q} = [r_Q(N + N_d - 1) \cdots r_Q(2N - 1)]^T$  and an  $(N - N_d + 1) \times N_d$  matrix  $\mathbf{R}_{2,I}$  with  $(i, j)$ th entry given by  $r_I(N + N_d - 1 + i - j)$ , which focus on the second block. From Fig. 2.5, signal after the I/Q imbalance compensation is written as

$$\tilde{\mathbf{r}}_i = (\mathbf{R}_{i,I} \mathbf{w} + \beta \mathbf{r}_{i,Q}) + j \mathbf{r}_{i,Q} \quad (4.4)$$

where  $i = 1, 2$  is the block index. Apparently, with the perfect imbalance compensation, we have  $\tilde{\mathbf{r}}_2 = e^{j(2\pi\theta)} \tilde{\mathbf{r}}_1$ . Substituting (4.4) into  $\tilde{\mathbf{r}}_2 = e^{j(2\pi\theta)} \tilde{\mathbf{r}}_1$ , we can write

$$\begin{cases} \mathbf{r}_{1,Q} \cos(2\pi\theta) + \mathbf{R}_{1,I} \mathbf{w} \sin(2\pi\theta) + \beta \mathbf{r}_{1,Q} \sin(2\pi\theta) = \mathbf{r}_{2,Q} \\ -\mathbf{r}_{1,Q} \sin(2\pi\theta) + \mathbf{R}_{1,I} \mathbf{w} \cos(2\pi\theta) + \beta \mathbf{r}_{1,Q} \cos(2\pi\theta) = \mathbf{R}_{2,I} \mathbf{w} + \beta \mathbf{r}_{2,Q} \end{cases} \quad (4.5)$$

Recalling from Sec. 2.4, we see that with perfect compensation, we have to choose  $\beta = \tan(\phi)$  and  $w(n) = \frac{\epsilon}{\cos\phi} g_d(n)$ . Substituting the first equation into the second one of (4.5) to eliminate  $\mathbf{r}_{2,Q}$ , we have

$$\mathbf{r}_{1,Q} = \underbrace{\begin{bmatrix} \mathbf{R}_{1,I} & \mathbf{R}_{2,I} \end{bmatrix}}_{\mathbf{\Lambda}} \underbrace{\begin{bmatrix} (-\sin\phi + \frac{\cos\phi \cos 2\pi\theta}{\sin 2\pi\theta}) \epsilon \mathbf{g}_d \\ -\frac{\cos\phi}{\sin 2\pi\theta} \epsilon \mathbf{g}_d \end{bmatrix}}_{\mathbf{q}_1} \quad (4.6)$$

Similarly, substitute the second equation into the first equation of (4.5) to eliminate  $\mathbf{r}_{1,Q}$ . We have

$$\mathbf{r}_{2,Q} = \underbrace{\begin{bmatrix} \mathbf{R}_{1,I} & \mathbf{R}_{2,I} \end{bmatrix}}_{\mathbf{\Lambda}} \underbrace{\begin{bmatrix} (\sin(2\pi\theta - \phi) + \frac{\cos(2\pi\theta - \phi) \cos 2\pi\theta}{\sin 2\pi\theta}) \epsilon \mathbf{g}_d \\ -\frac{\cos(2\pi\theta - \phi)}{\sin 2\pi\theta} \epsilon \mathbf{g}_d \end{bmatrix}}_{\mathbf{q}_2} \quad (4.7)$$

When  $N \geq 3N_d - 1$ ,  $\mathbf{\Lambda}$  is a tall matrix. Therefore, we can use the least-square algorithm to obtain  $\mathbf{q}_1$  and  $\mathbf{q}_2$  as

$$\mathbf{q}_1 = \mathbf{\Lambda}^\dagger \mathbf{r}_{1,Q} \quad (4.8)$$

$$\mathbf{q}_2 = \mathbf{\Lambda}^\dagger \mathbf{r}_{2,Q} \quad (4.9)$$

where  $\mathbf{\Lambda}^\dagger$  is the pseudo-inverse of  $\mathbf{\Lambda}$ . From the definition of  $\mathbf{q}_1$  and  $\mathbf{q}_2$  in (4.6) and (4.7), we have  $q_1(n) - q_2(n + N_d) = \frac{2 \cos\phi \cos 2\pi\theta}{\sin 2\pi\theta} \epsilon g_d(n)$  where  $0 \leq n < N_d$ . From the second half of  $\mathbf{q}_1$  in (4.6), we can write the equation as follows:

$$-2q_1(n + N_d) \cos 2\pi\theta = (q_1(n) - q_2(n + N_d))$$

We can estimate  $\cos 2\pi\theta$  by the well-known LLS algorithm.

$$\widehat{\cos 2\pi\theta} = \mathbf{u}^\dagger \mathbf{v} \quad (4.10)$$

where  $\mathbf{u} = -2[q_1(N_d) \cdots q_1(2N_d - 1)]^T$  and  $\mathbf{v} = [(q_1(0) - q_2(N_d)) \cdots (q_1(N_d - 1) - q_2(2N_d - 1))]^T$ . However, due to cosine function, the estimation range of CFO is limited to  $0 < \theta < 0.5$ .

**Solving the polarity ambiguity of  $\theta$ :** To extend the range of  $\theta$  of the estimator, obtaining  $\text{sign}\{\sin 2\pi\theta\}$  is necessary. Let  $n_0$  be a delay parameter so that  $g_d(n_0)$  has the maximum magnitude and it is positive. From the definition of  $\mathbf{q}_1$  and  $\mathbf{q}_2$  in (4.6) and (4.7),

$$n_0 = \arg \max_{0 \leq n < n_d} \{|q_1(n)| + |q_1(n + N_d)| + |q_2(n)| + |q_2(n + N_d)|\} \quad (4.11)$$

Because  $\phi$  is an small angle and  $\epsilon \approx 1$ , the assumption  $\epsilon \cos \phi > 0$  is reasonable. Moreover, from the definition of  $\mathbf{q}_1$  and  $\mathbf{q}_2$  in (4.6) and (4.7), the second equal sign in the below equation is held.

$$\begin{aligned} \text{sign}\{\sin 2\pi\theta\} &= \text{sign}\{\epsilon \cos \phi \sin 2\pi\theta\} \\ &= \text{sign}\left\{q_2(n_0) + q_2(n_0 + N_d) \widehat{\cos 2\pi\theta} - \widehat{\cos 2\pi\theta} \left(\frac{q_1(n_0) + q_2(n_0 + N_d)}{2}\right)\right\} \end{aligned} \quad (4.12)$$

According (4.10) and (4.12), the estimation range is extended to  $0.5 > \theta > -0.5$ . However, there is still one problem in this algorithm. Because of the property of cosine function, the performance is getting worse when  $2\pi\theta \approx 0$  or  $\pi$ . In what follows, we will show how to solve this problem.

**Refinement of the CFO estimate:** From (2.28), the received signal after CP removed can be written as

$$r(n) = \Re\{e^{j\frac{2\pi n\theta}{N}} [x(n) \otimes_c h(n)]\} + j\Im\{e^{j\frac{2\pi n\theta}{N}} [x(n) \otimes_c h(n) \otimes_c g'_d(n)]\} \quad (4.13)$$

where  $g'_d(n) = \epsilon e^{j(\phi - \frac{2\pi n\theta}{N})} g_d(n)$ . We can estimate the equivalent channel  $h(n)$  from the real part of  $r(n)$ . The real part of the above equation is given by

$$\hat{\mathbf{r}}_{1,I} = \begin{bmatrix} \Re\{\mathbf{E}(\theta)\mathbf{X}_c\} & -\Im\{\mathbf{E}(\theta)\mathbf{X}_c\} \end{bmatrix} \begin{bmatrix} \Re\{\mathbf{h}\} \\ \Im\{\mathbf{h}\} \end{bmatrix} \quad (4.14)$$

where  $\mathbf{r}_{1,I} \triangleq [r_I(0) \ r_I(1) \ \cdots \ r_I(N-1)]$ ;  $\mathbf{E}(\theta) = \text{diag}[1 \ e^{j\frac{2\pi\theta}{N}} \ \cdots \ e^{j\frac{2\pi(N-1)\theta}{N}}]$ ;  $\mathbf{h} = [h(0) \ h(1) \ \cdots \ h(N_h - 1)]^T$ ; and  $\mathbf{X}_c$  is an  $N \times N_h$  circulant matrix with the first column is  $[x(0) \ x(1) \ \cdots \ x(N-1)]^T$ . From (4.14), we see that given  $\theta$ , we can obtain the channel response from  $\mathbf{r}_{1,I}$ . Thus, given an estimate of CFO in (4.10) and (4.12), we can estimate  $\mathbf{h}$  in a least-squares sense:

$$\begin{bmatrix} \Re\{\hat{\mathbf{h}}\} \\ \Im\{\hat{\mathbf{h}}\} \end{bmatrix} = \mathbf{Y}^\dagger \mathbf{r}_{1,I} \quad (4.15)$$

where  $\mathbf{Y} = \begin{bmatrix} \Re\{\mathbf{E}(\hat{\theta}_1)\mathbf{X}_c\} & \Im\{\mathbf{E}(\hat{\theta}_1)\mathbf{X}_c\} \end{bmatrix}$  and  $\hat{\theta}_1$  is the estimated  $\theta$  from (4.10-4.12). Similarly, define  $\mathbf{r}_{2,I} \triangleq [r(N) \ r(N+1) \ \cdots \ r(2N-1)]$ . Thus, we write the real part of  $\mathbf{r}_2$  as

$$\mathbf{r}_{2,I} = \cos 2\pi\theta \mathbf{r}_{1,I} - \sin 2\pi\theta \Im\{E(\theta)\mathbf{X}_c\mathbf{h}\} \quad (4.16)$$

From (4.16), it is seen that  $\sin 2\pi\theta$  can be estimated from  $\mathbf{r}_{1,I}$ ,  $\mathbf{r}_{2,I}$ , and  $\Im\{E(\theta)\mathbf{X}_c\mathbf{h}\}$ . Substituting (4.15) into (4.16), we can estimate  $\sin 2\pi\theta$  using LLS algorithm. That is

$$\begin{bmatrix} \widehat{\cos 2\pi\theta} \\ \widehat{\sin 2\pi\theta} \end{bmatrix} = \mathbf{K}^\dagger \mathbf{r}_{2,I} \quad (4.17)$$

where  $\mathbf{K} = [\mathbf{r}_{1,I} \ -\Im\{\mathbf{E}(\hat{\theta}_1)\mathbf{X}_c\hat{\mathbf{h}}\}]$ .

We only take  $\widehat{\sin 2\pi\theta}$ . We abandon  $\widehat{\cos 2\pi\theta}$  of 4.17 since it is found to be less accurate than  $\widehat{\cos 2\pi\theta}$  of (4.10). In summary, combining (4.10-4.12) and (4.17),  $\theta$  is estimated by

$$\hat{\theta} = \frac{\arctan \frac{\widehat{\sin 2\pi\theta}}{\widehat{\cos 2\pi\theta}}}{2\pi} \quad (4.18)$$

### 4.1.2 I/Q Imbalance Estimation

In *GPP* method, while  $\sin(\eta + \Omega) = 0$ , we cannot estimate the compensation filter  $w(n)$ . In this subsection, we propose an algorithm to estimate I/Q mismatch and the performance will not get worse for any particular  $\theta$ . To do this, we define an

$(2N - N_d + 1) \times N_d$  matrix

$$\mathbf{Z} = \begin{bmatrix} z(N_d - 1) & z(N_d - 2) & \cdots & z(0) \\ z(N_d) & z(N_d - 1) & \cdots & z(1) \\ \vdots & \vdots & \ddots & \vdots \\ z(2N - 1) & z(2N - 2) & \cdots & z(2N - N_d) \end{bmatrix}, \quad (4.19)$$

where  $z(n) = e^{j\frac{2\pi n\theta}{N}} [x(n) \otimes_c h(n)]$ . Note that  $z(n)$  depends on  $\theta$  and  $\mathbf{h}$ . We have  $\hat{\theta}$  from (4.20) in previous subsection. We can estimate  $\mathbf{h}$  from real component of  $r(n)$  using LLS algorithm. That is

$$\begin{bmatrix} \Re\{\hat{\mathbf{h}}\} \\ \Im\{\hat{\mathbf{h}}\} \end{bmatrix} = \mathbf{Y}^\dagger \begin{bmatrix} \hat{\mathbf{r}}_{1,I} \\ \hat{\mathbf{r}}_{2,I} \end{bmatrix} \quad (4.20)$$

where

$$\mathbf{Y} = \begin{bmatrix} \Re\{\mathbf{E}(\hat{\theta})\mathbf{X}_c\} & -\Im\{\mathbf{E}(\hat{\theta})\mathbf{X}_c\} \\ \Re\{e^{j2\pi\hat{\theta}}\mathbf{E}(\hat{\theta})\mathbf{X}_c\} & -\Im\{e^{j2\pi\hat{\theta}}\mathbf{E}(\hat{\theta})\mathbf{X}_c\} \end{bmatrix} \quad (4.21)$$

According to (4.13), we have

$$\mathbf{r}_Q = \Im\{ee^{-j\phi}\mathbf{Z}\mathbf{g}_d\} \quad (4.22)$$

$$= \Re\{\mathbf{Z}\}\Im\{ee^{-j\phi}\mathbf{g}_d\} + \Im\{\mathbf{Z}\}\Re\{ee^{-j\phi}\mathbf{g}_d\} \quad (4.23)$$

where  $\mathbf{r}_Q = [r_Q(N_d - 1) \ r_Q(N_d) \ \cdots \ r_Q(2N - 1)]^T$ . (4.23) can be rewritten as

$$\mathbf{r}_Q = \underbrace{\begin{bmatrix} \Im\{\mathbf{Z}\} & \Re\{\mathbf{Z}\} \end{bmatrix}}_{\mathbf{A}(\theta, h)} \begin{bmatrix} \Re\{ee^{-j\phi}\mathbf{g}_d\} \\ \Im\{ee^{-j\phi}\mathbf{g}_d\} \end{bmatrix} \quad (4.24)$$

Apparently, the estimated  $ee^{-j\phi}\mathbf{g}_d$  is given by

$$\begin{bmatrix} \Re\{\widehat{ee^{-j\phi}\mathbf{g}_d}\} \\ \Im\{\widehat{ee^{-j\phi}\mathbf{g}_d}\} \end{bmatrix} = \mathbf{A}^\dagger(\hat{\theta}, \hat{h})\mathbf{r}_Q \quad (4.25)$$

where  $\hat{\theta}$  comes from (4.20);  $\hat{h}$  comes from (4.20). It's easy to derive  $\hat{\beta}$  and  $\hat{\mathbf{w}}$  from (4.25). We have

$$\hat{\beta} = -(\Re\{\widehat{ee^{-j\phi}\mathbf{g}_d}\})^\dagger (\Im\{\widehat{ee^{-j\phi}\mathbf{g}_d}\}) \quad (4.26)$$

$$\hat{\mathbf{w}} = \frac{\Re\{\widehat{ee^{-j\phi}\mathbf{g}_d}(n)\} + j\Im\{\widehat{ee^{-j\phi}\mathbf{g}_d}(n)\}}{e^{-j\hat{\phi}} \cos \hat{\phi}} \quad (4.27)$$

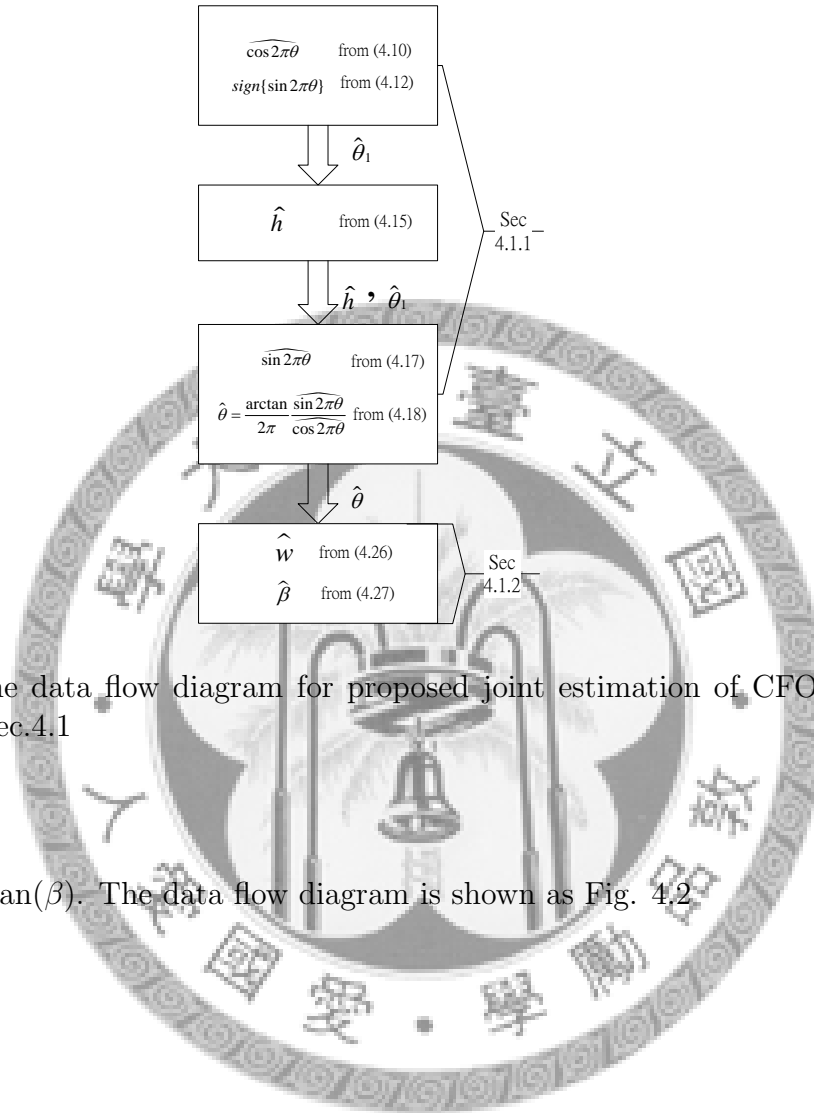


Figure 4.2: The data flow diagram for proposed joint estimation of CFO and I/Q imbalance in Sec.4.1

where  $\hat{\phi} = \arctan(\beta)$ . The data flow diagram is shown as Fig. 4.2

## 4.2 Improved of GPP Method

Because of using accos function, the performance of the CFO estimator is worse when  $(\eta + \Omega) \approx 0$  or  $\pm\pi$ . An better way is to find  $\sin(\eta + \Omega)$ , therefore, we can use the arctan to replace accos in the closed form of CFO estimation. Actually, it is reasonable to use the training sequence in Fig.4.1, which is more generous. In the GPP method, the minimum of the cost function in (3.6) is achieved when (4.5) holds, we rewrite

(3.10) as

$$\underbrace{\mathbf{\Lambda} \begin{bmatrix} \cos 2\pi\theta + \beta \sin 2\pi\theta \\ \cos 2\pi\theta - \beta \sin 2\pi\theta \\ \mathbf{w} \sin 2\pi\theta \end{bmatrix}}_{\mathbf{q}} = \begin{bmatrix} \mathbf{r}_{2,Q} \\ \mathbf{r}_{1,Q} \end{bmatrix} \quad (4.28)$$

where

$$\mathbf{\Lambda} = \begin{bmatrix} \mathbf{r}_{1,Q} & \mathbf{0} & \mathbf{R}_{1,I} \\ \mathbf{0} & \mathbf{r}_{2,Q} & -\mathbf{R}_{2,I} \end{bmatrix} \quad (4.29)$$

and  $\mathbf{0}$  is a  $(N - N_d + 1) \times 1$  all-zero vector. When  $N \geq 2N_d - 1$ ,  $\mathbf{\Lambda}$  is a tall matrix. Therefore, it is able to calculate

$$\mathbf{q} = \mathbf{\Lambda}^\dagger \begin{bmatrix} \mathbf{r}_{2,Q} \\ \mathbf{r}_{1,Q} \end{bmatrix} \quad (4.30)$$

by well-known LLS algorithm. As shown in (3.13), we have a closed-form solution for CFO estimation:

$$\hat{\theta} = \frac{\arccos \left( \frac{q(0) + q(1)}{2} \right)}{2\pi} \quad (4.31)$$

As described in previous section, if  $\Omega = \pi/2$ , the CFO estimation range is  $\theta \in (-\frac{N}{4K}, \frac{N}{4K})$  in GPP method. The training sequence in this section can be considered as a case of  $\Omega = 0$  and  $K = N$ . Hence, the CFO estimation range is  $\theta \in (0, 0.5)$ . It is necessary to know  $\text{sign}\{\sin 2\pi\theta\}$  for extending the estimation range to  $\theta \in (-0.5, 0.5)$ . It is reasonable to assume that the peak of  $w(n)$  is positive. Thus, we can find out

$$\text{sign}\{\sin 2\pi\theta\} = \text{sign}\{q(n_0)\} \quad (4.32)$$

where

$$n_0 = \arg \max_{2 \leq n < N_d + 1} \{|q(n)|\} \quad (4.33)$$

In short, we can estimate fractional  $\theta$  from (4.31) and (4.32). The compensation filter  $w(n)$  and  $\beta$  can be observed from  $q(n)$ . That is

$$\hat{\mathbf{w}} = \frac{1}{\sin 2\pi\hat{\theta}} [q(3) \ q(4) \ \cdots \ q(N_d + 1)]^T \quad (4.34)$$

$$\hat{\beta} = \frac{q(0) - q(1)}{2 \sin 2\pi\hat{\theta}} \quad (4.35)$$

Using (4.31) to (4.35), the signal after the I/Q imbalance compensation can be rewrite as

$$\tilde{\mathbf{r}}_i = (\mathbf{R}_{i,I}\hat{\mathbf{w}} + \hat{\beta}\mathbf{r}_{i,Q}) + j\mathbf{r}_{i,Q} \quad (4.36)$$

A refinement of the CFO is described as below. We will estimate  $\theta$  using the property  $\tilde{\mathbf{r}}_2 = e^{j(2\pi\theta)} \tilde{\mathbf{r}}_1$ . An autocorrelation-based CFO estimator can then be applied to the compensated samples, generating CFO estimates

$$\hat{\theta} = \frac{\angle(\tilde{\mathbf{r}}_1^\dagger \tilde{\mathbf{r}}_2)}{2\pi} \quad (4.37)$$

### 4.3 Improved of Three-Block method

There are two problems with the CFO estimation method in Sec. 3.2. One is the phase ambiguity problem as the range of  $\theta$  in the estimator is limited to  $[0.5, 0]$ . The other is that, when  $\theta \approx 0$  or  $0.5$ , the estimation error of  $\theta$  increases rapidly.

**Solving the ambiguity of  $\theta$ :** To extend the estimation range of  $\theta$ , we have to know the  $\text{sign}\{\sin 2\pi\theta\}$ . It is easy to verify that

$$\tilde{r}_I(n+2N) - \tilde{r}_I(n) = -2\tilde{r}_Q(n+N) \sin 2\pi\theta \quad (4.38)$$

$$\tilde{r}_Q(n+2N) - \tilde{r}_Q(n) = 2\tilde{r}_I(n+N) \sin 2\pi\theta \quad (4.39)$$

where  $\tilde{\mathbf{r}}_i$  are the samples via compensation structure.

Substituting (4.4) into (4.38),(4.39) can be written as

$$\mathbf{r}_{3,Q} - \mathbf{r}_{1,Q} = 2 \sin 2\pi\theta (\mathbf{R}_{2,I}\mathbf{w} - \beta\mathbf{r}_{2,Q}) \quad (4.40)$$

Using LLS algorithm, we can estimate  $\sin 2\pi\theta\mathbf{w}$  from (4.40) Define  $\mathbf{Y} \triangleq [\mathbf{R}_{2,I} \ \mathbf{r}_{2,Q}]$ .

We have

$$\begin{bmatrix} \widehat{\sin 2\pi\theta\mathbf{w}} \\ \widehat{\sin 2\pi\theta\beta} \end{bmatrix} = \mathbf{Y}^\dagger (\mathbf{r}_{3,Q} - \mathbf{r}_{1,Q}) \quad (4.41)$$

We assume  $w(n_0)$  has the maximum magnitude and it is positive, where  $n_0 = \arg \max_{0 \leq n < n_d-1} \{|\widehat{\sin 2\pi\theta w(n)}|\}$ . Thus,

$$\text{sign}\{\sin 2\pi\theta\} = \text{sign}\{\widehat{\sin 2\pi\theta w(n_0)}\} \quad (4.42)$$



Overall, we extend the range of  $\hat{\theta}$  in (3.22) to  $-0.5 < \theta < 0.5$ .

**Refinement of the CFO estimate:** To solve the second problem, a complementary sine estimator is generally needed. From Sec. 4.1.2, the I/Q mismatch can be compensated by given  $\theta$ . Consequently, the sine estimator can be obtained from (4.38) and (4.39).  $\tilde{r}_i$  ( $i=1, 2, 3$ ) is obtain by substituting (4.34) and (4.35) into (4.4). Given  $\tilde{r}_i$  we can obtain a sine CFO estimate as

$$\widehat{\sin 2\pi\theta} = \tilde{\mathbf{u}}^\dagger \tilde{\mathbf{v}} \quad (4.43)$$

where

$$\tilde{\mathbf{u}} = 2 \begin{bmatrix} \tilde{r}_I(N) \\ \tilde{r}_I(N+1) \\ \vdots \\ \tilde{r}_I(2N-1) \\ -\tilde{r}_Q(N) \\ -\tilde{r}_Q(N+1) \\ \vdots \\ -\tilde{r}_Q(2N-1) \end{bmatrix} \quad (4.44)$$

and

$$\tilde{\mathbf{v}} = \begin{bmatrix} \tilde{r}_Q(2N) - \tilde{r}_Q(0) \\ \tilde{r}_Q(2N+1) - \tilde{r}_Q(1) \\ \vdots \\ \tilde{r}_Q(3N-1) - \tilde{r}_Q(N-1) \\ \tilde{r}_I(2N) - \tilde{r}_I(0) \\ \tilde{r}_I(2N+1) - \tilde{r}_I(1) \\ \vdots \\ \tilde{r}_I(3N-1) - \tilde{r}_I(N-1) \end{bmatrix} \quad (4.45)$$

Combining (3.22) and (4.43), the CFO  $\theta$  is given by

$$\hat{\theta} = \frac{\arctan\left(\frac{\widehat{\sin 2\pi\theta}}{\widehat{\cos 2\pi\theta}}\right)}{2\pi} \quad (4.46)$$

The data flow diagram is shown as Fig. 4.3

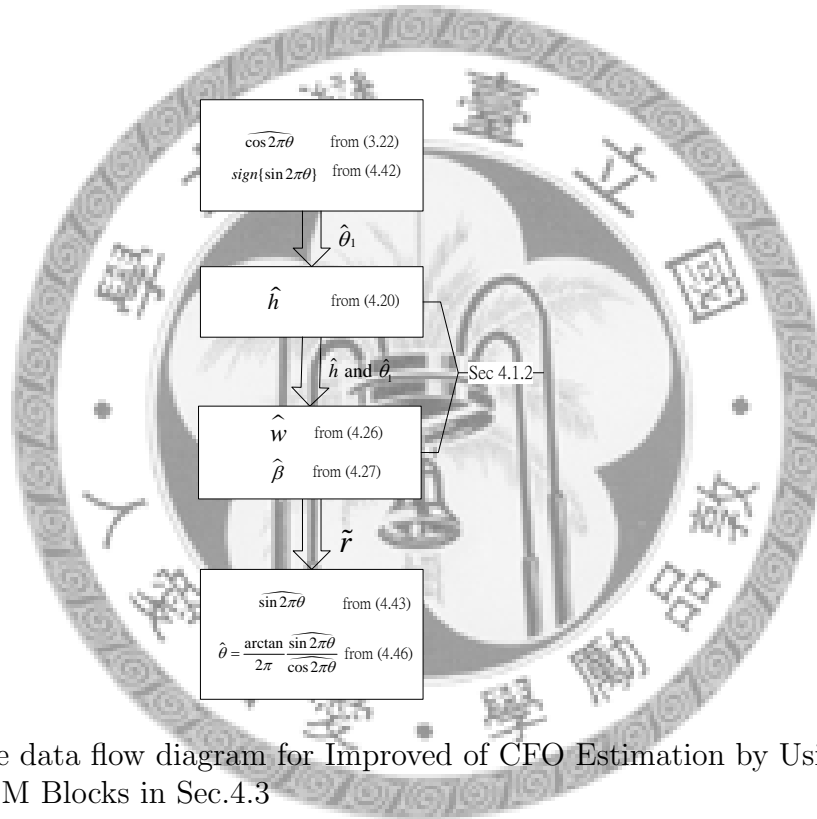


Figure 4.3: The data flow diagram for Improved of CFO Estimation by Using Three Repeated OFDM Blocks in Sec.4.3

## 4.4 Simulation Results and Comparison

In this section, we carry out Monte Carlo experiments to show the performance comparison of the estimation methods which introduced in chapter 3 and chapter 4. The channel is quasi-static with order  $N_c = 4$  and the length of CP  $L$  satisfies  $L > N_h - 1$ , so that there are no IBI after the CP removal. Channel taps are independent and identically distribution (i.i.d.) complex Gaussian random variables and the variance of the channel taps is normalized by  $\sum_{n=0}^{N_c} \mathbb{E}\{|c(n)|^2\} = 1$ . Assume that the noise is AWGN with noise power  $\mathcal{N}_0$ , and the modulated symbols are QPSK with symbol power  $\mathcal{E}_s$ . The SNR is defined as  $\mathcal{E}_s/\mathcal{N}_0$ . The size of the DFT matrix is  $N = 64$ . We consider the I/Q imbalance scenario in [16], where the amplitude and phase mismatches are  $\epsilon = 5dB$  and  $\phi = 5^\circ$ . The LPF of I-branch and Q-branch are  $\mathbf{g}_I = [1 \ 0.1]^T$  and  $\mathbf{g}_Q = [1 \ -0.1]^T$  respectively. As the result, the ideal  $g_d(n)$  is IIR filter. We assume that  $w(n)$  has 5 taps ( $N_d = 5$ ) for containing 98% of energy, i.e. the ideal  $\mathbf{w} = [w(0) \ w(1) \ \dots \ w(N_d - 1)]^T = \frac{\epsilon}{\cos\phi} [1 \ -0.2 \ 0.02 \ -0.002 \ 0.0002]^T$ . The estimation MSE is defined as

$$MSE(\theta) = \frac{1}{K} \sum_{i=1}^K |\hat{\theta}^{(i)} - \theta|^2 \quad (4.47)$$

$$MSE(\beta) = \frac{1}{K} \sum_{i=1}^K |\hat{\beta}^{(i)} - \beta|^2 \quad (4.48)$$

$$MSE(\mathbf{w}) = \frac{1}{K} \sum_{i=1}^K \|\hat{\mathbf{w}}^{(i)} - \mathbf{w}\|^2 \quad (4.49)$$

where  $\hat{\theta}$ ,  $\hat{\beta}$  and  $\hat{\mathbf{w}}$  represent the estimated  $\theta$ ,  $\beta$  and  $\mathbf{w}$  respectively.  $\hat{\theta}^i$ ,  $\hat{\beta}^i$  and  $\hat{\mathbf{w}}^i$  stand for the estimated value in  $i$ th trial. A total of  $K=2000$  trials are used in the experiment.

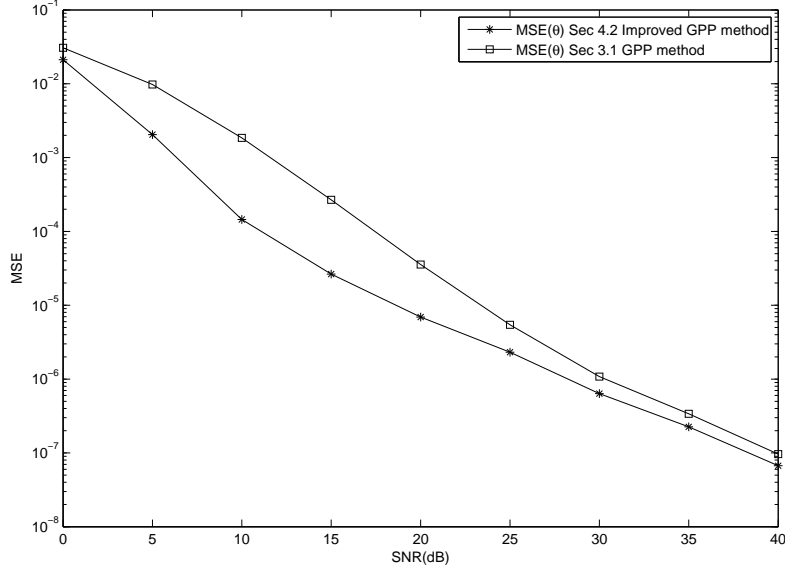


Figure 4.4: Example 4.1. MSE for the estimation of CFO versus SNR ( $\theta = 0.3072$ )

**Example 4.1** In this example, we show the performance comparison of the GPP method in Sec. 3.1 and Improved GPP method in Sec 4.2. Consider the wireless LAN system of *IEEE802.11a* with carrier frequency 5.2GHz,  $N = 64$  subcarriers, and bandwidth 20MHz. The GPP is generated by adding phase rotate to the short preamble of this system, which corresponds to  $M = 10$  and  $K = 16$ . The phase difference  $\Omega$  is set to  $\pi/2$  as in [13]. The SNR is defined by the ratio of the signal power to the variance of channel noise. The GPP method employs  $P = K(M - 2) = 128$ .

As shown in Figure 4.4, we compare the MSE of estimated  $\theta$  versus SNR. The CFO is set to  $\Delta f = 96kHz$ , i.e.  $\theta = 0.3072$ . Both algorithm decrease the  $MSE(\theta)$  as SNR gets large. The  $MSE(\theta)$  of our Improved GPP method is better than [13].

Figure 4.5 shows the performance for MSE of estimated CFO versus different value of  $\theta$ . The constant SNR is 30dB. We can see that Improved GPP method is much better than GPP, especially for large CFO value. The reason is that GPP using a arcos estimator, but Improved GPP using a arctan estimator. Notice that for this

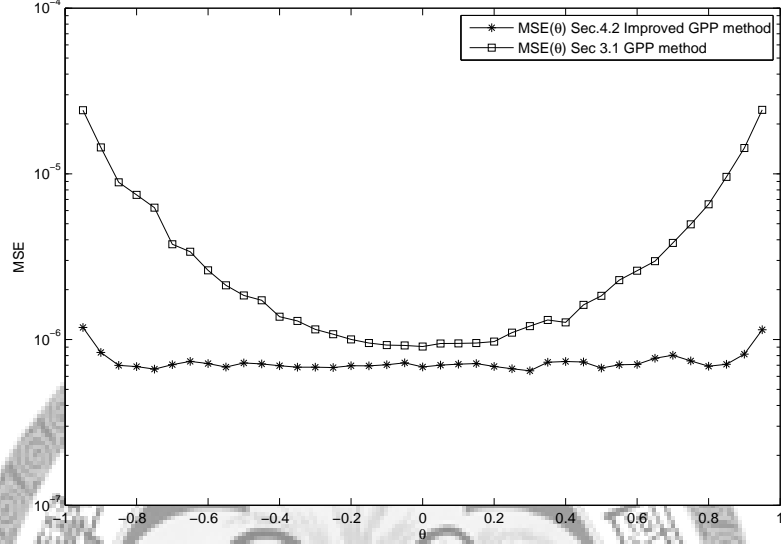
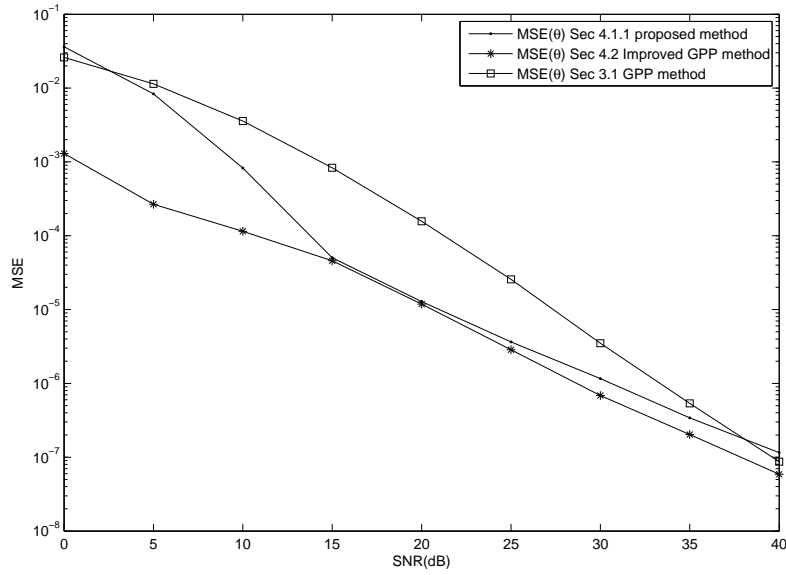
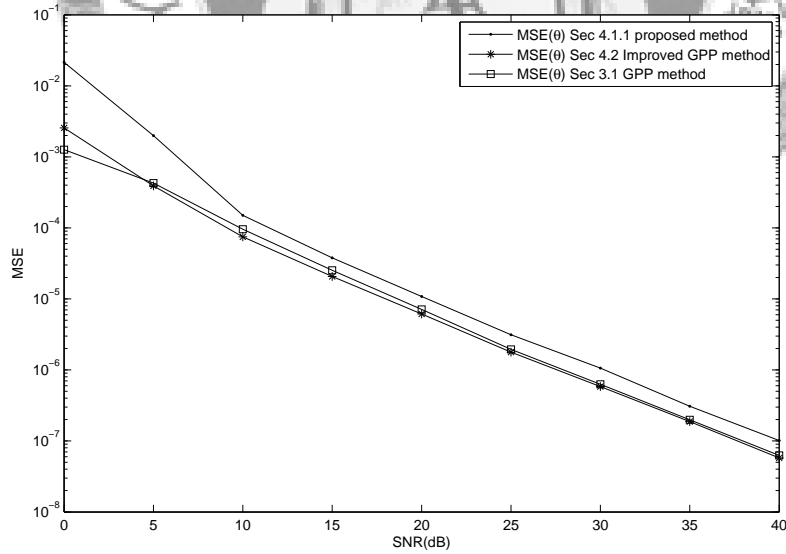


Figure 4.5: Example 4.1. MSE for the estimation of  $\theta$  versus different CFO parameter

preamble, the CFO estimation range of GPP method is  $\theta \in (-1, 1)$ . However the range of Improved GPP method is  $\theta \in (-2, 2)$ .

**Example 4.2** In this example, we show the performance comparison of the GPP method, Improved GPP method and proposed method. There are two identical OFDM blocks of preamble in the system. Therefore, the GPP method employs  $\Omega = 0$ . Notice the CP of training sequence is longer enough to avoid IBI.

We compare the MSE of estimated  $\theta$  versus SNR. As shown in Figure 4.6 and Figure 4.7, we consider that  $\theta = 0.02$  and  $\theta = 0.2$ , respectively. All the algorithms decrease the  $MSE(\theta)$  as SNR gets large in Figure 4.6 and Figure 4.7. Furthermore, Improved GPP method is always better than GPP method and proposed method. When  $\theta$  is small, it is obvious that  $MSE(\theta)$  of proposed GPP method is better than GPP method as shown in Figure 4.6. However, when  $\theta = 0.2$ , our proposed method is worse than GPP method.

Figure 4.6: Example 4.2. MSE for the estimation of CFO versus SNR ( $\theta = 0.02$ )Figure 4.7: Example 4.2. MSE for the estimation of CFO versus SNR ( $\theta = 0.2$ )

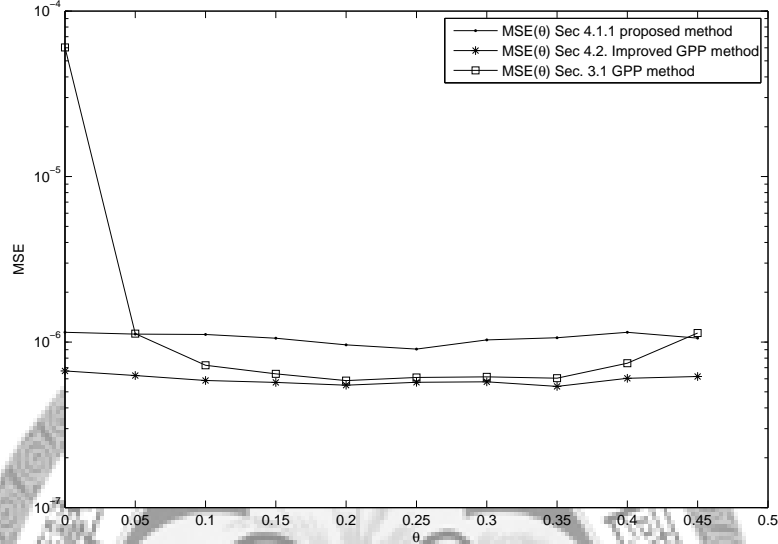


Figure 4.8: Example 4.2. MSE for the estimation of  $\theta$  versus different CFO parameter

Figure 4.8 shows the performance for MSE of estimated CFO versus different value of  $\theta$ . The constant SNR is 30dB. We can see that Improved GPP method is much better than GPP in any  $\theta$ . The performance of our proposed method is less about 2dB than GPP in most case, but when  $\theta$  is around zero, the performance of our method is much better than GPP. Notice that for this preamble, the CFO estimation range of GPP method is  $\theta \in (0, 0.5)$ . Furthermore the range of both proposed method and Improved GPP method is  $\theta \in (-0.5, 0.5)$ .

**Example 4.3** In this example, we show the performance comparison of proposed method in Sec 4.1 and the GPP method in Sec 3.1. There are two identical OFDM blocks of preamble in the system. Therefore, the GPP method employs  $\Omega = 0$ . Notice the CP of training sequence is longer enough to avoid IBI.

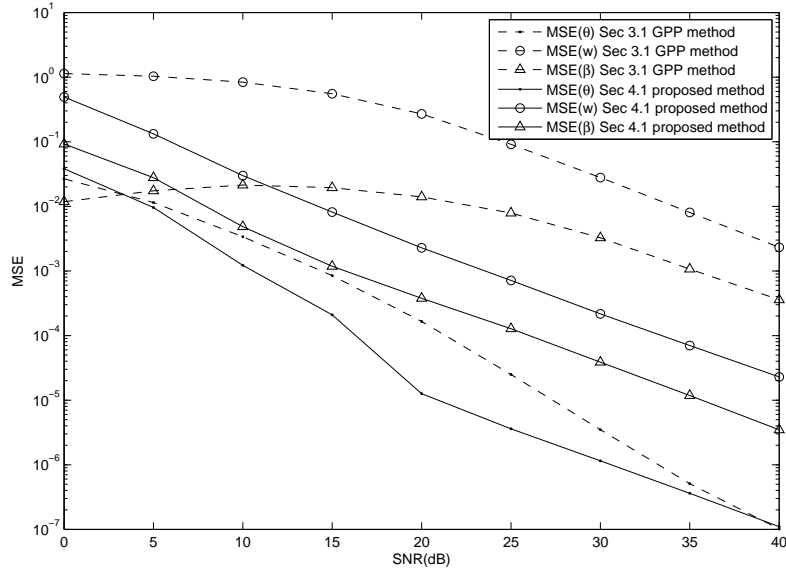


Figure 4.9: Example 4.3. MSE for the estimation of CFO versus SNR ( $\theta = 0.02$ )

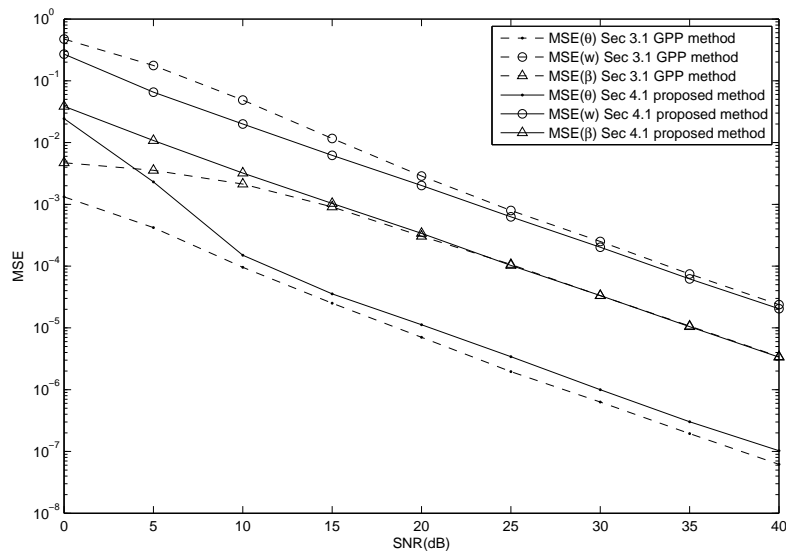


Figure 4.10: Example 4.3. MSE for the estimation of CFO versus SNR ( $\theta = 0.2$ )



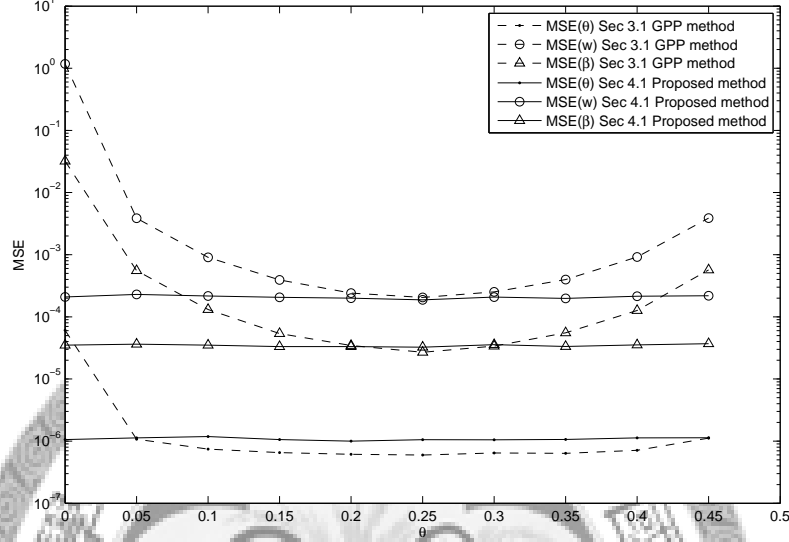


Figure 4.11: Example 4.3. MSE for the estimation of  $\theta$  versus different CFO parameter

AS shown in Fig. 4.10, We consider  $\theta = 0.02$ .  $MSE(\mathbf{w})$ ,  $MSE(\beta)$  and  $MSE(\theta)$  of proposed method is better than GPP. The performance of  $MSE(\theta)$  of proposed method is close to GPP in high SNR.

AS shown in Fig. 4.10, We consider  $\theta = 0.2$ .  $MSE(\mathbf{w})$  of proposed method is better than GPP, but  $MSE(\beta)$  of proposed method is worse than GPP in low SNR. The performance of I/Q imbalance is very close in high SNR.  $MSE(\theta)$  of proposed method is worse than GPP, especially the low SNR.

AS shown in Fig. 4.11, We consider  $SNR = 30dB$ .  $MSE(\mathbf{w})$  and  $MSE(\beta)$  of proposed method is better than GPP.  $MSE(\beta)$  of proposed method is close to  $MSE(\beta)$  of GPP when  $0.2 < \theta < 0.3$ .  $MSE(\theta)$  of proposed method is worse about 2dB than  $MSE(\theta)$  of GPP for most  $\theta$ . However the performance of  $MSE(\theta)$  for proposed method is much better than GPP when  $\theta$  is small.

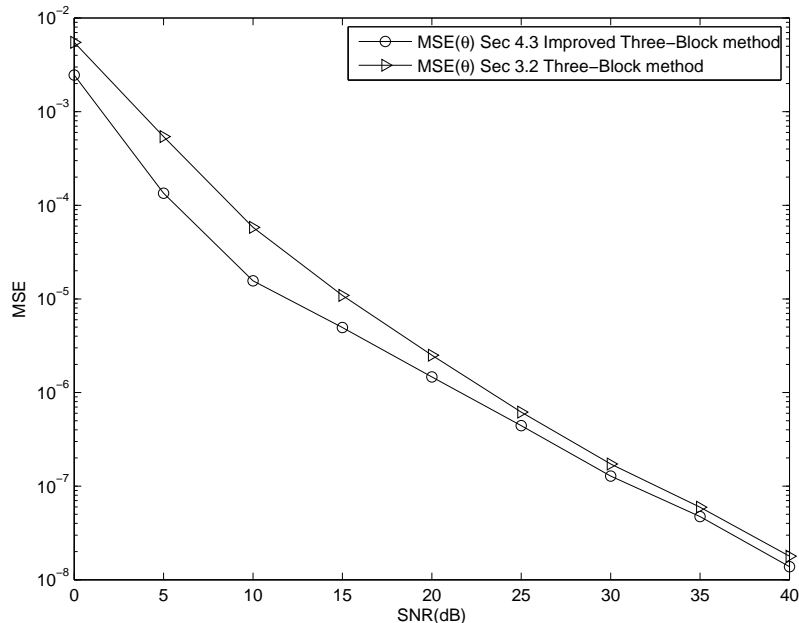


Figure 4.12: Example 4.4. MSE for the estimation of CFO versus SNR ( $\theta = 0.2$ )

**Example 4.4** In this example, we show the performance comparison of Three-Blocks CFO estimation method in Sec. 3.3 and Improved Three-Blocks CFO estimation method in Sec 4.3. There are three identical OFDM blocks of preamble in the system. Notice the CP of training sequence is longer enough to avoid IBI.

As shown in Figure 4.12, we compare the MSE of estimated  $\theta$  versus SNR. The CFO is set to  $\theta = 0.2$ . Both algorithm decrease the  $MSE(\theta)$  as SNR gets large. It is obvious that  $MSE(\theta)$  of Improved Three-Blocks method is better than Three-Blocks method.

Figure 4.13 shows the performance for MSE of estimated CFO versus different value of  $\theta$ . The constant SNR is 30dB. We can see that Improved Three-Blocks method is much better than Three-Blocks method in any  $\theta$ . Remark that for this preamble, the CFO estimation range of Three-Blocks method is  $\theta \in (0, 0.5)$ . Furthermore the range of the Improved Three-Blocks method is  $\theta \in (-0.5, 0.5)$ .

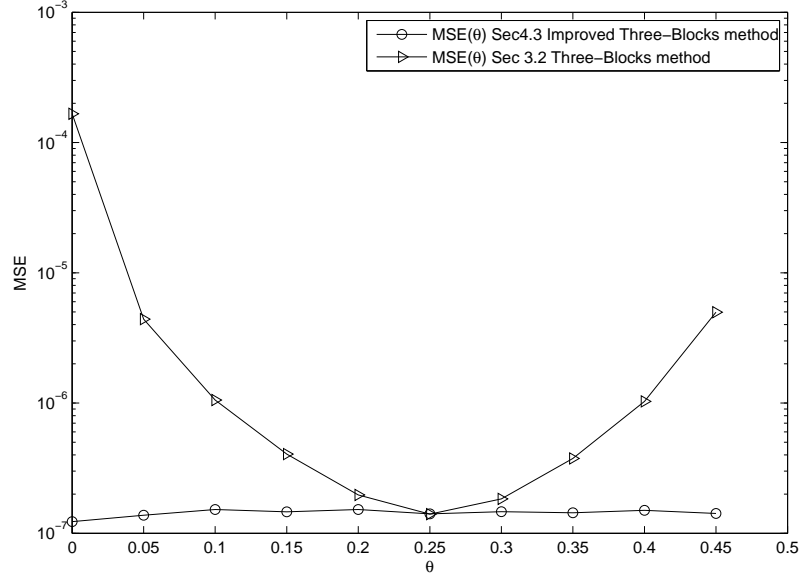


Figure 4.13: Example 4.4. MSE for the estimation of  $\theta$  versus different CFO parameter

**Example 4.5** In this example, we show the performance comparison of the GPP method, Improved GPP method, Three-Block method and Improved Three-Block method. Consider the wireless LAN system of *IEEE802.11a* with carrier frequency 5.2GHz,  $N = 64$  subcarriers, and bandwidth 20MHz. All the algorithm have the same short preamble of this system, which corresponds to  $M = 10$  and  $K = 16$ . There are no phase shift between two symbols (i.e.,  $\Omega = 0$ ). The SNR is defined by the ratio of the signal power to the variance of channel noise. The GPP method and Improved GPP employ  $P = K(M - 2) = 128$ .

As shown in Figure 4.14, we compare the MSE of estimated  $\theta$  versus SNR. The CFO is set to  $\Delta f = 96kHz$ , i.e.  $\theta = 0.3072$ . All the algorithms decrease the  $MSE(\theta)$  as SNR gets large. We can see that All the improved methods is better than the original methods. Furthermore, Improved Three-Blocks method is better than Improved GPP method.

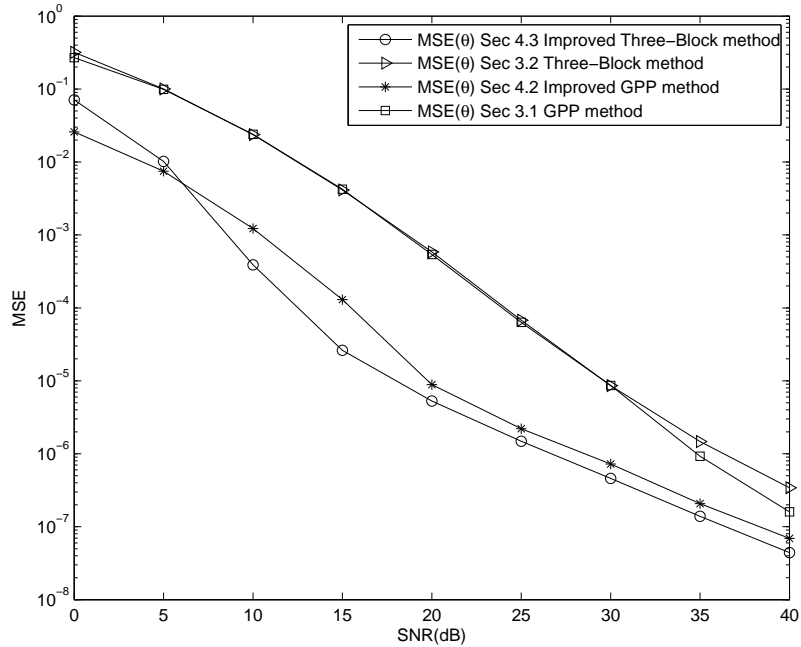
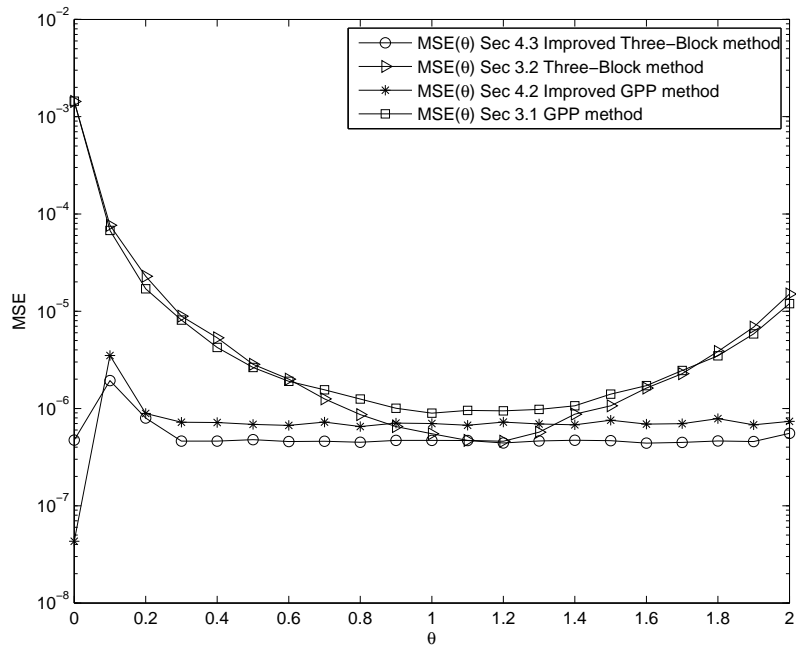
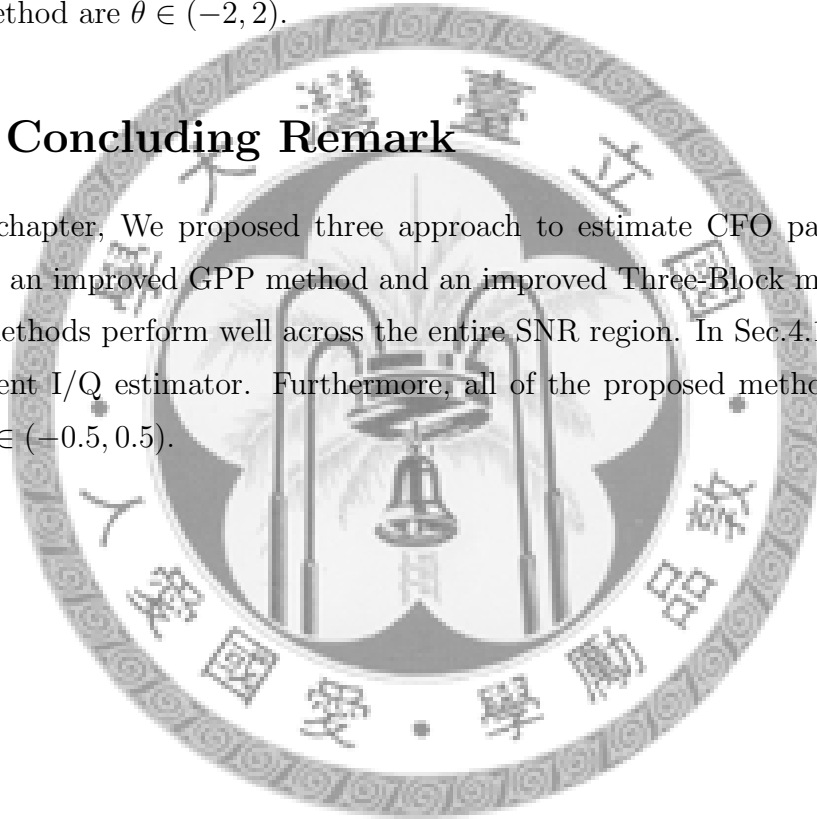
Figure 4.14: Example 4.5. MSE for the estimation of CFO versus SNR ( $\theta = 0.3072$ )Figure 4.15: Example 4.5. MSE for the estimation of  $\theta$  versus different CFO parameter

Figure 4.15 shows the performance for MSE of estimated CFO versus different value of  $\theta$ . The constant SNR is 30dB. We can see that All the improved methods is better than the original methods,especially when  $\theta \approx 0$ . Furthermore, Improved Three-Blocks method is better than Improved GPP method. Remark that for this preamble, the CFO estimation range of Three-Blocks method and GPP method are  $\theta \in (0, 2)$ . Furthermore the range of the Improved Three-Blocks method, Improved GPP method are  $\theta \in (-2, 2)$ .

## 4.5 Concluding Remark

In this chapter, We proposed three approach to estimate CFO parameter: a new method, an improved GPP method and an improved Three-Block method. The proposed methods perform well across the entire SNR region. In Sec.4.1.2, we proposed an efficient I/Q estimator. Furthermore, all of the proposed methods perform well when  $\theta \in (-0.5, 0.5)$ .





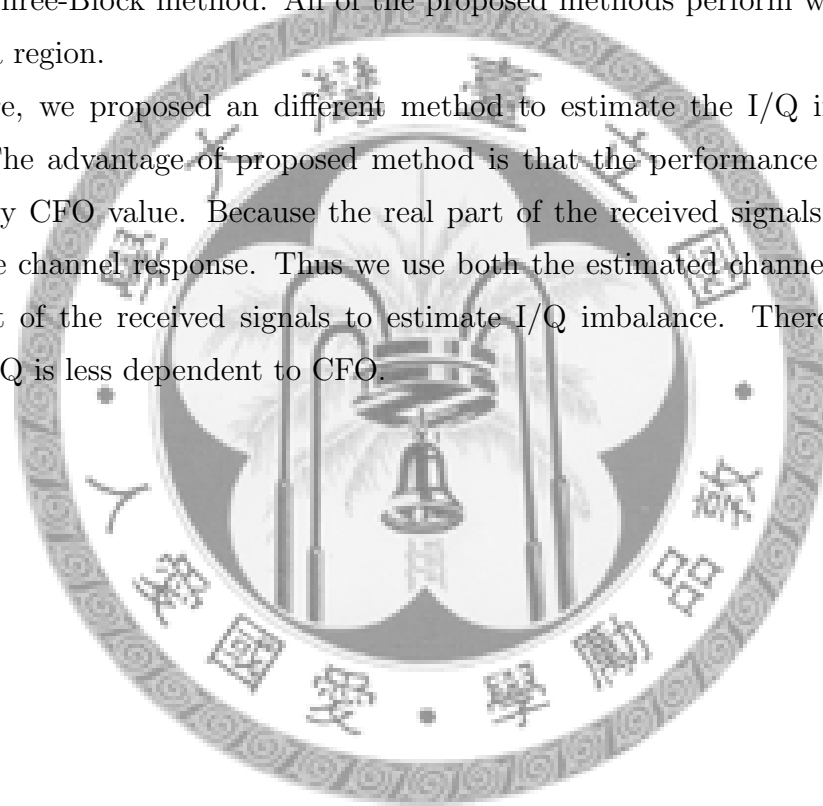
## Chapter 5

## Conclusion



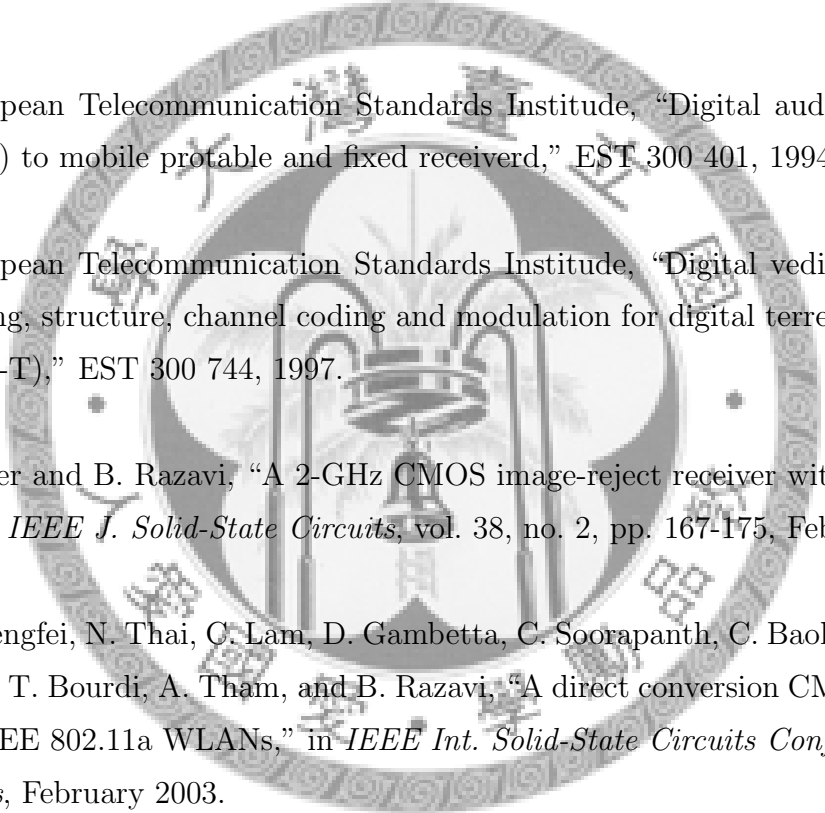
In OFDM systems, the presence of I/Q imbalance and CFO cause the performance to degrade considerably. In this thesis, joint estimation of I/Q imbalance, CFO and channel response was presented. The method we proposed is performed in the time domain and requires a preamble, which is arbitrary and does not have to satisfy any pattern. We have no constraint on the channel response. We proposed three approaches to estimate CFO parameter: a new method, an improved GPP method and an improved Three-Block method. All of the proposed methods perform well across the entire SNR region.

Furthermore, we proposed a different method to estimate the I/Q imbalance parameters. The advantage of the proposed method is that the performance does not fail well for any CFO value. Because the real part of the received signals are used to estimate the channel response. Thus we use both the estimated channel and the imaginary part of the received signals to estimate I/Q imbalance. Therefore, the estimator of I/Q is less dependent to CFO.





# Bibliography

- 
- [1] European Telecommunication Standards Institute, “Digital audio broadcasting (DAB) to mobile portable and fixed receiverd,” EST 300 401, 1994.
- [2] European Telecommunication Standards Institute, “Digital vedio broadcasting; framing, structure, channel coding and modulation for digital terrestrial television (DVB-T),” EST 300 744, 1997.
- [3] L. Der and B. Razavi, “A 2-GHz CMOS image-reject receiver with LMS calibration,” *IEEE J. Solid-State Circuits*, vol. 38, no. 2, pp. 167-175, February 2003.
- [4] Z. Pengfei, N. Thai, C. Lam, D. Gambetta, C. Soorapanth, C. Baohong, S. Hart, I. Sever, T. Bourdi, A. Tham, and B. Razavi, “A direct conversion CMOS transceiver for IEEE 802.11a WLANs,” in *IEEE Int. Solid-State Circuits Conf. Dig Technical papers*, February 2003.
- [5] Darryl Dexu Lin, Ryan A. Pacheco, Teng Joon Lim, and Dimitrios Hatzinakos, “Joint estimation of channel response, frequency offset, and phase noise in OFDM,” *IEEE Transactions on Signal Processing*, vol. 54, no. 9, September 2006.
- [6] Qiyue Zou, Alireza Tarighat, and Ali H. Sayed, “Compensation of phase noise in OFDM wireless systems,” *IEEE Transactions on Signal Processing*, vol. 55, no. 11, November 2007.

- [7] Songping Wu, and Yehekel Bar-Ness, "OFDM channel estimation in the presence of frequency offset and phase noise," *IEEE International Conference on Communications*, vol. 5, pp. 3366-3370, May 2003.
- [8] B. Razavi, *RF Microelectronics*. Englewood Cliffs, NJ: Prentice-Hall, 1998.
- [9] Yuan-Pei Lin and See-May Phoong, "BER minimized OFDM systems with channel independent precoders," , volume 51, issue 9, pp. 2369-2380, September 2003.
- [10] Li-Hsiang Lee, "Performance Study of OFDM and SC-CP Systems in Non-ideal Transmission Environment," *Master thesis, National Taiwan University*, June 2005.
- [11] M. J. M. Pelgrom, A. C. J. Duinmaijer, and A. P. G. Welbers, "Matching properties of MOS transistors," *IEEE J. Solid-State Circuits*, vol. 24, no. 5, pp. 1433-1439, October 1989.
- [12] Guanbin Xing, Manyuan Shen, and Hui Liu, "Frequency Offset and I/Q Imbalance Compensation for Direct-Conversion Receivers," *IEEE Transactions on Wireless Communication*, vol. 4, no. 2, March 2005.
- [13] Hai Lin, Xu Zhu, and Katsumi Yamashita, "Low-Complexity Pilot-Aided Compensation for Carrier Frequency Offset and I/Q imbalance," *IEEE Transactions on Communications*, vol. 58, no. 2, February 2010.
- [14] Ying Chen, Jian(Andrew) Zhang, and A.D.S.Jayalath, "Low-Complexity Estimation of CFO and Frequency Independent I/Q Mismatch for OFDM systems," *EURASIP Journal on Wireless Communications and Networking*, Volume 2009.
- [15] Yuan-Hwui Chung, "Estimation and Compensation of Front-end Nonidealities in OFDM Systems," *Doctoral Dissertation, National Taiwan University*, July, 2009.

- [16] Balachander Narasimhan, Sudharsan Narayanan, Hlaing Minn, Naofal Al-Dhahir, "Reduced-Complexity Baseband Compensation of Joint Tx/Rx I/Q Imbalance in Mobile MIMO-OFDM," *IEEE Transactions on Wireless Communication*, vol. 9, no. 5, May 2010.

